NASA CONTRACTOR REPORT

NASA CR-2054

CAVITATION IN LIQUID CRYOGENS

I — Venturi

by J. Hord, L. M. Anderson, and W. J. Hall

Prepared by
NATIONAL BUREAU OF STANDARDS
Boulder, Colo. 80302
for Lewis Research Center

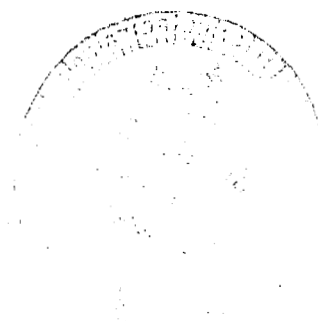

NATIONAL AERONAUTICS AND SPACE ADMINISTRATION • WASHINGTON, D. C. • MAY 1972

1. Report No.	2. Government Accession No.	3. Recipient's Catalog No.
CR-2054		

4. Title and Subtitle	5. Report Date
CAVITATION IN LIQUID CRYOGENS I - VENTURI	May 1972
	6. Performing Organization Code
7. Author(s)	8. Performing Organization Report No.
J. Hord, L. M. Anderson, and W. J. Hall	None
	10. Work Unit No.
9. Performing Organization Name and Address	
National Bureau of Standards Boulder, Colorado 80302	11. Contract or Grant No. C-39004B
	13. Type of Report and Period Covered
12. Sponsoring Agency Name and Address	Contractor Report
National Aeronautics and Space Administration Washington, D.C. 20546	14. Sponsoring Agency Code

15. Supplementary Notes

Project Manager, Werner R. Britsch, Fluid System Components Division, NASA Lewis Research Center, Cleveland, Ohio

16. Abstract

This document constitutes the first of four volumes to be issued on the results of continuing cavitation studies. It is an extension of a previous study that defined the cavitation characteristics of liquid hydrogen and liquid nitrogen flowing in a transparent plastic venturi. Thermodynamic data, consisting of pressure and temperature measurements within fully developed hydrogen cavities, are reported here. These newer, more precise data essentially confirm the original data. Details concerning test apparatus, test procedure, and data correlation techniques are given.

17. Key Words (Suggested by Author(s))		18. Distribution Statement
Cavitation	Pumps	Unclassified - unlimited
Cryogenics	Venturi	
Nucleation		

19. Security Classif. (of this report)	20. Security Classif. (of this page)	21. No. of Pages	22. Price*
Unclassified	Unclassified	88	$3.00

* For sale by the National Technical Information Service, Springfield, Virginia 22151

1. Cavitation
2. Cryogenics
3. Cryopumping

CONTENTS

LIST OF FIGURES

LIST OF FIGURES (Continued)

LIST OF TABLES

CAVITATION IN LIQUID CRYOGENS

I - VENTURI

J. Hord, L. M. Anderson, and W. J. Hall

1. SUMMARY

This document constitutes the first of four volumes to be issued on the results of continuing cavitation studies. It is an extension of a previous study that defined the cavitation characteristics of liquid hydrogen and liquid nitrogen flowing in a transparent plastic venturi. Thermodynamic data, consisting of pressure and temperature measurements within fully developed hydrogen cavities, are reported here. In the previous study, it was concluded that the measured temperatures and pressures within the central and aft regions of the cavities were generally not in stable thermodynamic equilibrium. Because these results were not anticipated, it was decided that additional, more precise tests were in order. Accordingly, the plastic venturi has been equipped with additional pressure and temperature sensing ports, the temperature instrumentation improved, and additional tests performed. The new data positively confirm the older data. The cavity pressure depressions (bulkstream vapor pressure less measured cavity pressure) increased with increasing velocities, cavity length, and fluid temperature. Minimum measured cavity pressure was less than bulkstream vapor pressure by as much as 15.13 psi (10.44 N/cm^2); measured temperatures and pressures within the vaporous hydrogen cavities substantiated thermodynamic metastability in the central regions and trailing edges.

Existing correlative theory is used to obtain equations that correlate the new (and old) experimental data for developed cavitation in liquid hydrogen. The new equations are shown to be compatible with the older data and with the work of others.

Details of the test apparatus, test model, instrumentation, test procedure, data analysis, and correlative techniques are discussed. Experimental data resulting from this study are presented in tabular form over the range of experimental temperatures, 35.77 to 41.36 R (19.87 to 22.98 K) and inlet velocities, 98.8 to 194.0 ft/s (30.1 to 59.1 m/s).

2. INTRODUCTION

Vaporous cavitation is the formation of the vapor phase within a flowing liquid, due to a reduction in pressure. Since the formation and collapse of vapor cavities alters flow patterns, cavitation may reduce the efficiency of pumping machinery [1][1] and reduce the precision of flow measuring devices. Collapse of these vapor cavities can also cause serious erosion damage [2] to fluid-handling equipment. While the non-cavitating performance of hydraulic equipment may be predicted from established similarity laws, cavitating performance is much more difficult to predict from fluid-to-fluid. Recent advances in this area have been made by NASA-LeRC personnel [3-5], but additional work is required to improve the current technique for predicting cavitating performance of equipment from fluid-to-fluid. The effects of fluid properties on cavitation performance are well recognized [6-15] and require more understanding to develop improved similarity relations [15] for equipment behavior. Considerably more knowledge is needed to extend this predictive capability from one piece of equipment to another, i.e., a more general predictive technique, applicable to equipment design, must include the effects of equipment geometry and size, in addition to fluid properties.

---

[1] Numbers in brackets indicate references at the end of this paper.

NASA has undertaken a program [1] to determine the cavitation characteristics of various hydrodynamic bodies and the thermodynamic behavior of different fluids, in an effort to obtain improved design criteria to aid in the prediction of cavitating pump performance. The experimental study described herein was conducted in support of this program.

In the original work [16], liquid hydrogen and liquid nitrogen were chosen as test fluids for the following reasons: (1) the ultimate goal of this program is to acquire sufficient knowledge to permit intelligent design of pumps for near-boiling liquids, and (2) predictive analyses indicated [1] that the physical properties of hydrogen and nitrogen make them particularly desirable test fluids. The objective of that study [16] was to determine the flow and thermodynamic conditions required to induce incipient and developed cavitation on the walls of a transparent plastic venturi, using liquid hydrogen and liquid nitrogen. The shape of the venturi was chosen to duplicate the test section used by NASA [15].

One of the most interesting results of the initial work [16] was the indication that thermodynamic metastability exists in the midregions of the vaporous hydrogen cavities. In those tests, the uncertainty of the cavity temperature measurements precluded accurate definition of the magnitude of metastability within the cavities. Although the earlier work [16] was in itself complete, the instrumentation was less than optimum. Consequently, it was necessary to increase the number of pressure and temperature sensing ports to more clearly define the pressure and temperature profiles within the cavities; also, recent advances in cryogenic thermocouple thermometry and high-speed data acquisition systems made it possible to rapidly and precisely measure temperature at several locations in the cavity. The plastic venturi has been equipped with additional sensing ports, the temperature instrumentation improved, and the hydrogen tests repeated; the results of these improved tests are

presented herein and they positively confirm the initial data. Pressure and temperature profiles within fully developed hydrogen cavities were measured and are referred to herein as developed cavitation data. Venturi inlet velocities were varied from 98.8 to 194 ft/s (30.1 to 59.1 m/s) and inlet temperatures ranged from 35.77 to 41.36 R (19.87 to 22.98 K). The bulkstream vapor pressure exceeds the measured cavity pressure and the saturation pressure corresponding to the measured cavity temperature; therefore, the measured pressure depressions and the pressure depressions corresponding to the measured temperature depressions within the cavity are called "pressure depressions." Alternatively, the pressure depression may be expressed in terms of its equivalent equilibrium "temperature depression."

A similarity equation has been developed [15] for correlating cavitation data for a particular test item from fluid-to-fluid; this correlation is also useful in extending the velocity and temperature range of data for any given fluid. The experimental data from this study have been used to evaluate the exponents on various terms in this correlating equation. These new data have also been correlated with the old data [16] using the similarity equation. All data reported here are intended to supplement that given in reference [16] and are tabulated in appendix A.

Test apparatus, test procedure, instrumentation, and data analysis are described in this paper for the sake of completeness and because they have been substantially improved since the initial work was reported [16].

3. EXPERIMENTAL APPARATUS

The facility used for this study consisted of a blow-down system with the test section located between the supply and receiver dewars; see figure 3.1. Dewars and piping were vacuum shielded to minimize heat transfer to the test fluid. Flow control was attained with a motorized

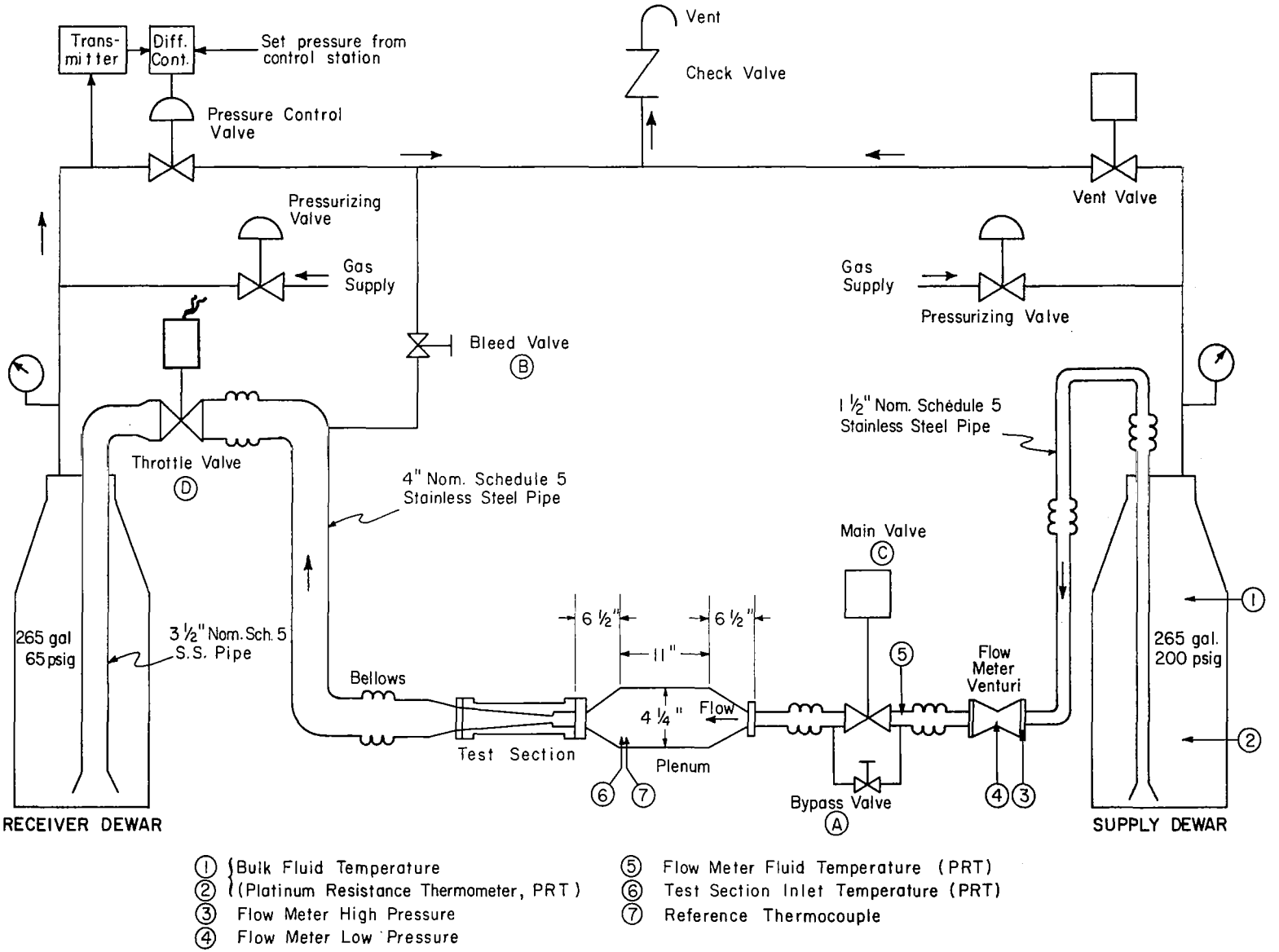

Figure 3.1 Schematic of cavitation flow apparatus.

throttle valve and by regulating the supply and receiver dewar pressures. Pressure and volume capacities of the supply and receiver vessels are indicated on figure 3. 1. The receiver dewar pressure control valving limited the inlet velocity, V_o, to around 200 ft/s (61 m/s) in these hydrogen tests. Valves located on each side of the test section permit flow stoppage in the event of venturi failure while testing with liquid hydrogen. A plenum chamber was installed upstream of the test section to assure uniform non-cavitating flow at the test section inlet. The supply dewar was equipped with a 5 kW heater which was used to heat the test fluid.

3. 1 Test Section

A photograph of the test section, as viewed through one of the windows in the vacuum jacket, is shown in figure 3. 2; this photograph was taken during the initial test series [16] and does not show the additional pressure and temperature sensing ports. The transparent plastic venturi was flanged into the apparatus using high compression elastomeric "O" rings. Test section details are given in figures 3. 3 and 3. 4. All but two of the sensing ports detailed in figure 3. 3 were used during the developed-cavity tests to determine the temperature and pressure depressions within the cavities. Sensor ports 3A and 3B were not used to avoid possible breakage of the plastic. Cavity length was determined from scribe marks on the plastic venturi; see figure 3. 2. The theoretical and as-built venturi contours are shown on figure 3. 4. The test section dimensions were checked by using the plastic venturi as a mold for a dental plaster plug. The plug was then removed and measured. Pressure distribution for non-cavitating flow across the quarter round contour [16 - 18] is shown in figure 3. 5. This pressure profile has been confirmed using several test fluids [15], and applies when $(Re)_{D_o} \geq 4 \times 10^5$.

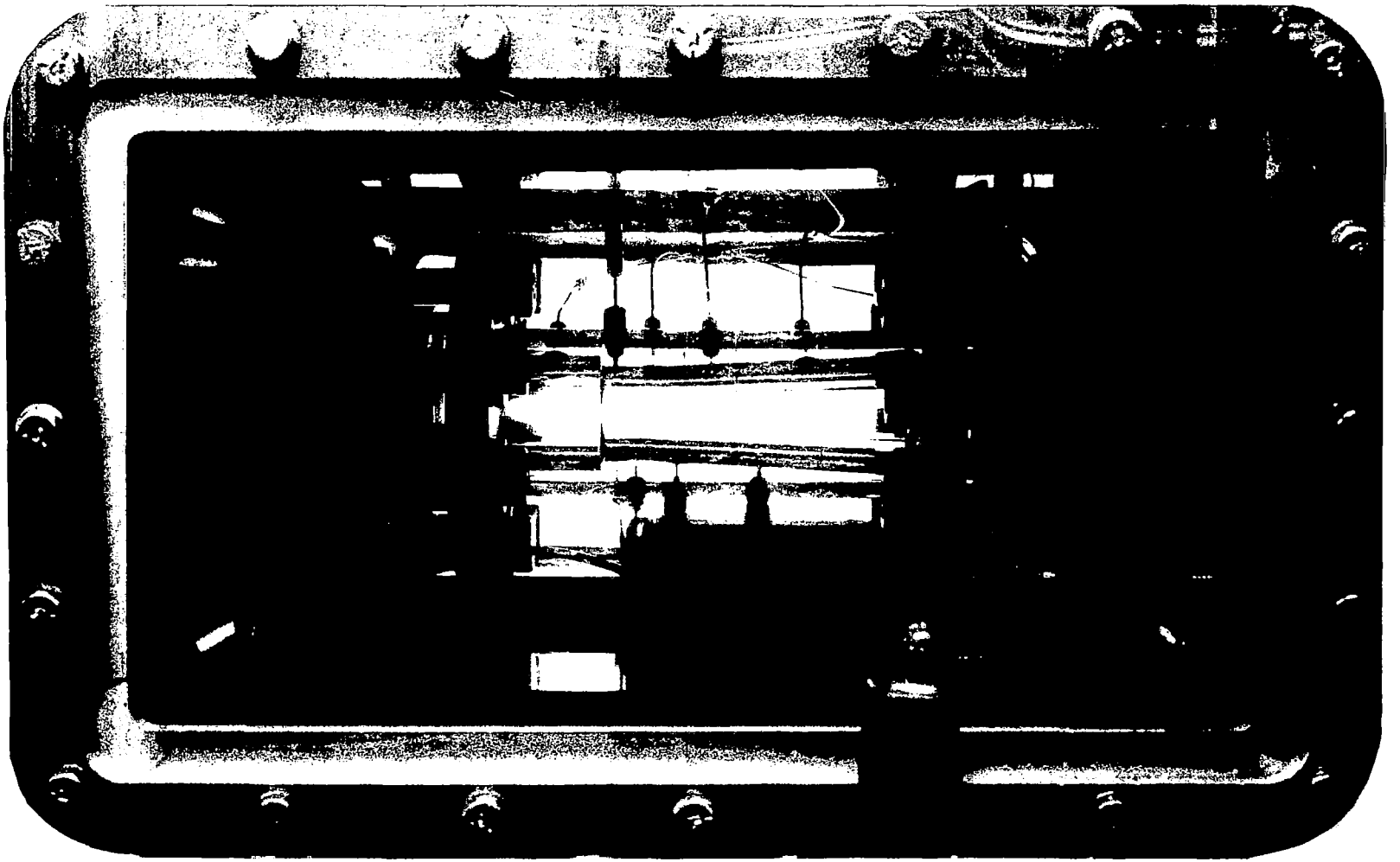

Figure 3.2 Photograph of plastic venturi test section installed in system. Note counter--used to correlate flow data with film event.

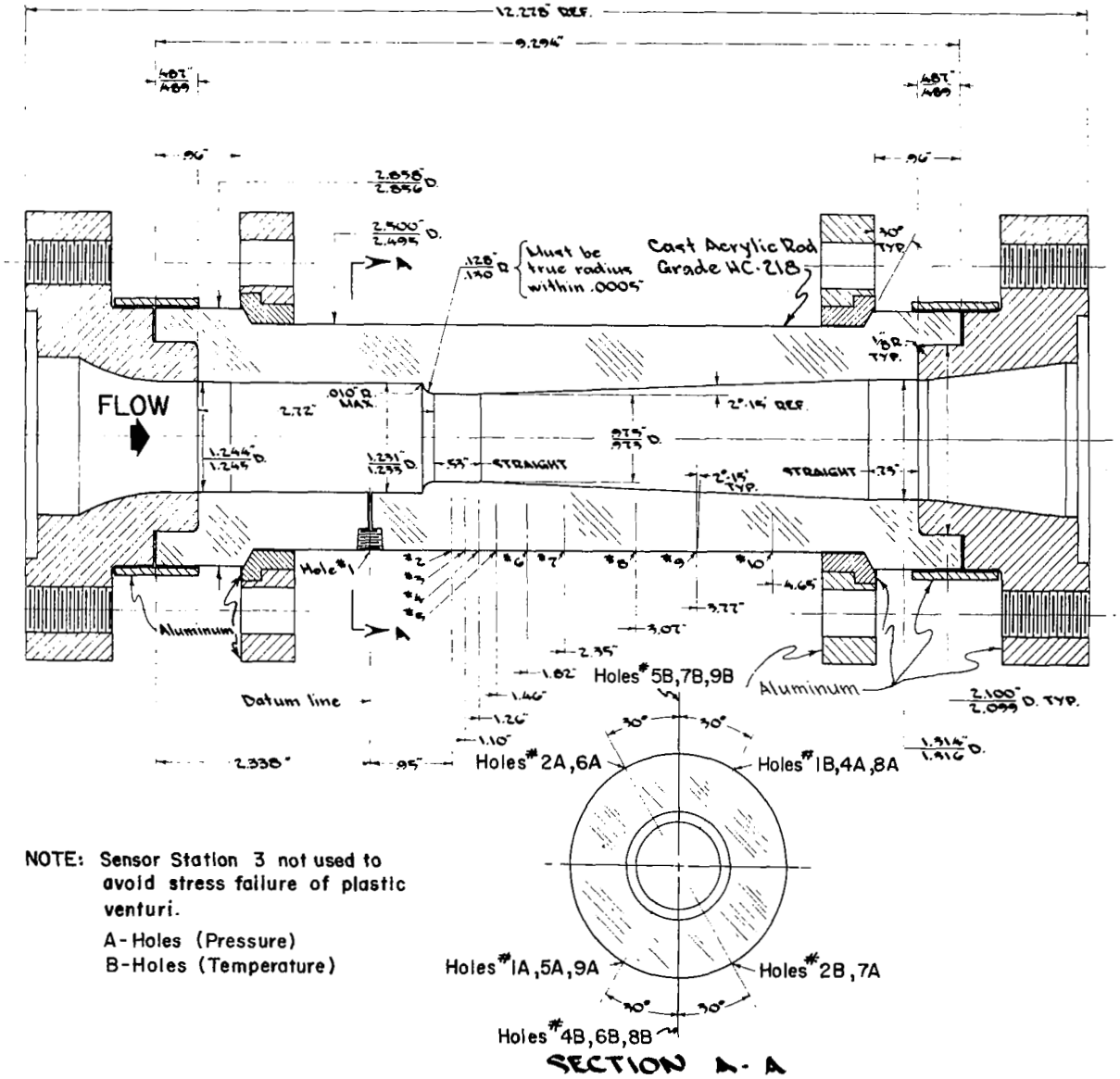

Figure 3.3 Sketch of plastic venturi section showing dimensions and location of pressure and temperature instrumentation.

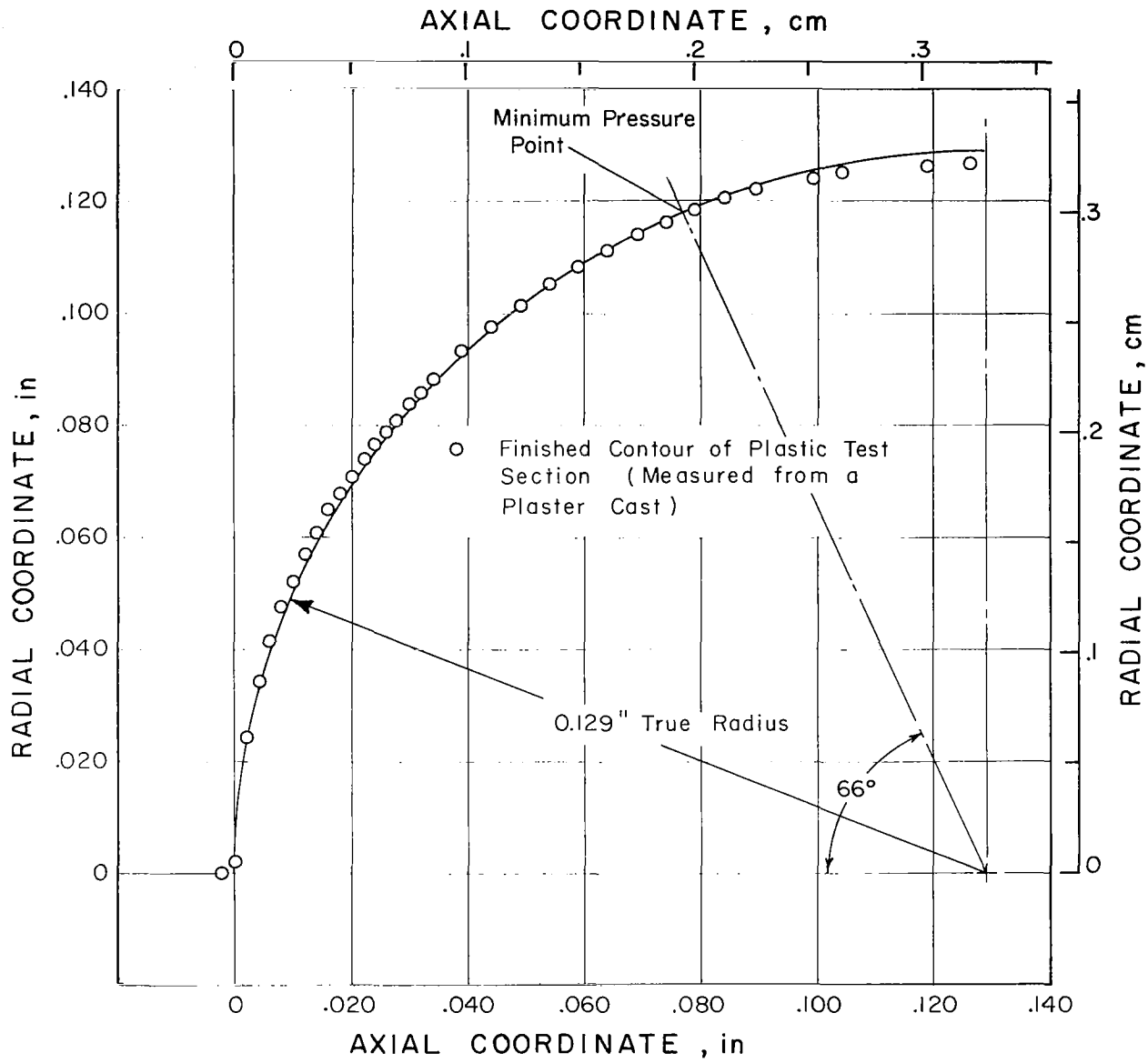

Figure 3.4 Quarter-Round contour of convergent region of plastic test section.

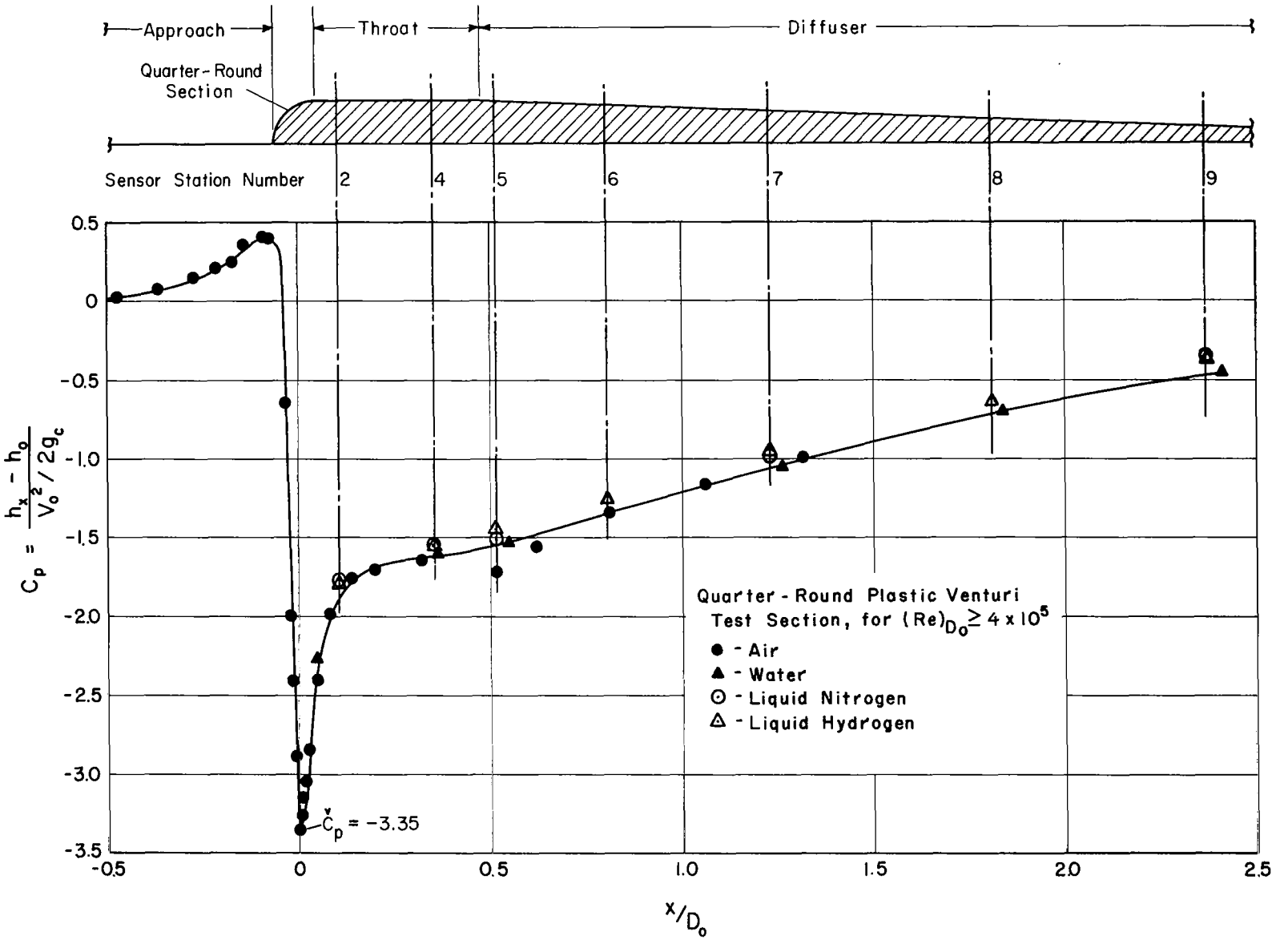

Figure 3.5 Pressure distribution through test section for non-cavitating flow.

3.2 Instrumentation

Location of the essential instrumentation is shown on figures 3.1 and 3.3. All of the error statements given in this section are based on an estimated systematic error and an estimated random error. The random error, or imprecision, has been assigned a 3 σ confidence limit, i.e., the random error cited will include 99.73 percent of the experimental observations.

Liquid level in the supply dewar was sensed with a ten-point carbon resistor rake. Test fluid temperature in the supply dewar was determined by two platinum resistance thermometers, see figure 3.1. Fluid temperature at the flowmeter and test section inlet were also measured with platinum resistance thermometers. These platinum thermometers were calibrated against a secondary thermometer standard and were powered with a current source that did not vary more than 0.01 percent. Voltage drop across the thermometers was recorded on a 4 digit electronic voltmeter data acquisition system. The overall uncertainty of the platinum thermometer temperature measurement is estimated to be within ± 0.09 R (± 0.05 K), with an allowance of ± 0.06 R (± .03 K) for systematic error and ± 0.03 R (± .02 K) for imprecision.

Chromel*-gold (0.07 atomic percent iron) thermocouples were used to determine the temperature profile within the cavities during the tests. These thermocouples more than double the signal voltage of the Chromel-constantan wires used in the initial study [16]. The reference thermocouples were placed in the plenum chamber beside the platinum thermometer used to determine bulkstream temperature at the test section inlet. The thermocouples had exposed soldered junctions and were constructed from 36 AWG wire to ensure rapid response. The detailed construction of these thermocouples is given in appendix B.

---

* Trade name --See footnote on page 58.

The thermocouple leads extending from the reference to cavity thermocouples were thermally lagged to the cold pipe and radiation shielded with multilayer aluminum foil. The signal leads which penetrated the vacuum barrier were also tempered to the cold pipe and radiation shielded to minimize heat transfer to the low temperature junctions. Details of the thermocouple installation are shown on figures 3.6 and 3.7. The thermocouple circuits were calibrated in situ, over the range of experimental velocities and temperatures, from tests involving non-cavitating flow through the venturi; i.e., pre and post calibrations were obtained during each developed-cavity test by causing non-cavitating flow to occur with only a slight variation in flow conditions. Overall uncertainty of the cavity temperature measurements is estimated at ± 0.36 R (± 0.20 K), with an allowance of ± 0.18 R (± 0.10 K) for systematic error and ± 0.18R (± 0.10 K) for imprecision.

System gage and differential pressure measurements were obtained with pressure transducers mounted in a temperature stabilized box near the test section. Differential pressure measurements were used where possible to provide maximum resolution. The pressure transducers were calibrated via laboratory test gages and manometers at frequent intervals during the test series. These transducers have a repeatability of better than ± 0.25 percent, and their output was recorded on a magnetic tape data acquisition system with better than ± 0.25 percent resolution. The overall uncertainty of the pressure measurements, including calibration and read-out errors, is estimated to be within ± 1.0 psi (± 0.69 N/cm^2), with an allowance of ± 0.2 psi (± 0.14 N/cm^2) for systematic error and ± 0.8 psi (±0.55 N/cm^2) for imprecision. Bourdon gauges were used to monitor the tests.

Volumetric and mass flow rates were determined via a Herschel venturi flow meter designed to ASME Standards [19]. The internal

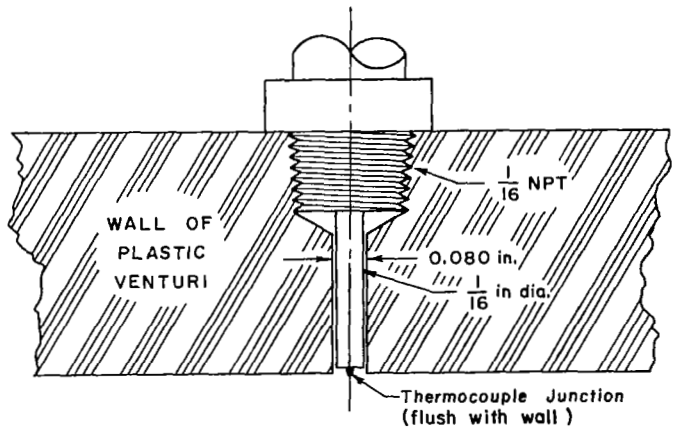

(.1): Detail of thermocouple instrument port

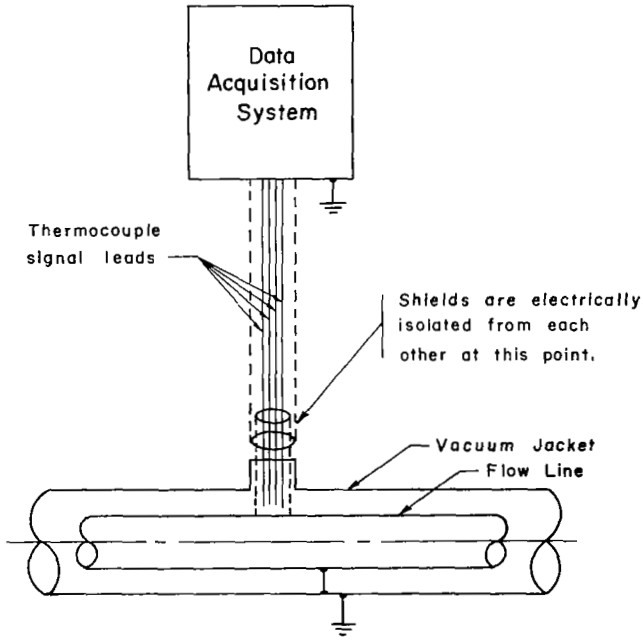

(.2): Schematic of thermocouple recording circuit

Figure 3.6 Installation and wiring details of thermocouples used to measure cavity temperatures.

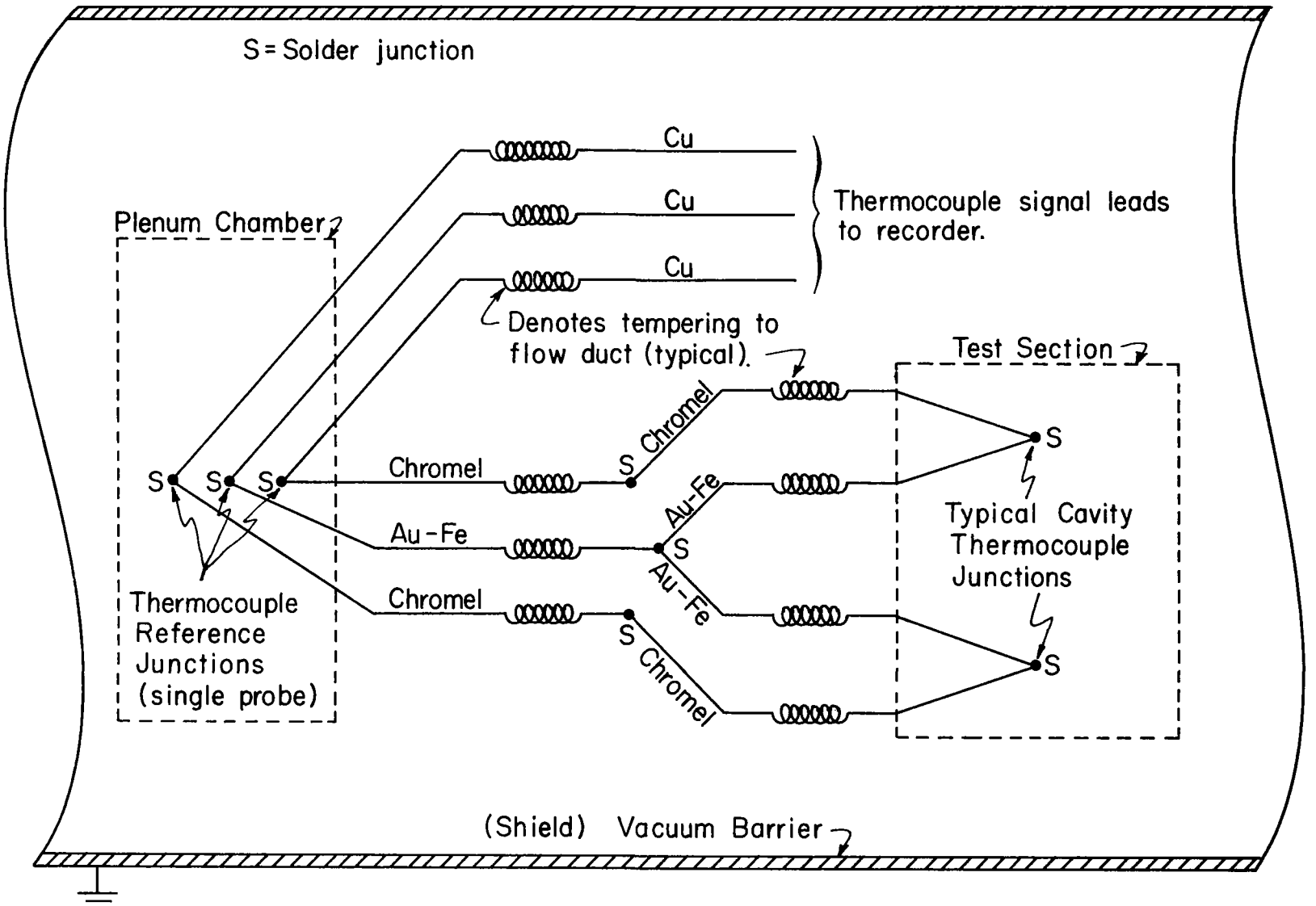

Figure 3.7 Schematic diagram of thermocouple measuring circuit, showing typical electrical connections for the thermocouples.

contour of this meter was verified in the same manner as the test venturi. An error analysis of this flow device and associated pressure and temperature measurements indicates an overall uncertainty in mass flow of ± 1.0 percent, with an allowance of ± 0.2 percent for systematic error and ± 0.8 percent for imprecision. The precision of the computed mass flow was periodically verified by comparison with the rate of efflux of liquid from the supply vessel; rate of efflux at low and intermediate flow rates was determined from liquid level-time measurements in the liquid level-volume-calibrated supply vessel.

An electronic pulsing circuit provided a common time base for correlating data between oscillograph (used for monitoring of tests), magnetic tape data acquisition system, and movie film. The electronic pulsing circuit was triggered by the scanner on the multi-channel data acquisition system. This 16 channel, magnetic tape recorder system was equipped with a multiplexor so that 32 data channels were sampled each second. Calibration information and data on the magnetic tape were subsequently used in a digital computer program to provide data for analysis. The data were reduced by first viewing film of the test event. A solenoid-actuated counter and a small light bulb, installed adjacent to the test section--see figure 3.2--were energized by the electronic pulser and appear on the film. Thus, the data retrieved from the magnetic tape are reduced at the desired instant of time by simply matching the number of voltage pulses which have elapsed.

3.3 Visual and Photographic Aids

Use of a plastic test section, liquid hydrogen, and relatively high pressures precluded direct visual observation; therefore, closed-circuit television was used to observe the tests.

Movies of cavitation tests were taken at approximately 20 frames per second on 16 mm film. The variable speed camera was equipped

with a 75 mm lens and synchronized with a high intensity stroboscope, providing a 3 microsecond exposure. The stroboscope was situated directly opposite the camera lens and illuminated the test section through a plastic diffuser mask; this technique provided bright field illumination or a back-lighting effect and excellent contrast between vapor and liquid phases in the test section. A low-intensity flood light was also used to provide continuous back-lighting for television reception.

4. TEST PROCEDURE

The following procedure refers to figure 3. 1. The supply dewar was filled with test liquid and then some of the liquid extracted through valves A and B to slowly cool the test section and piping. Approximately 2 hours were required to cool the plastic test section without breakage. Cooldown was monitored with the platinum resistance thermometer in the plenum chamber. Upon completion of cooldown, the remaining contents of the supply dewar were transferred through the test section into the receiver dewar, and then back into the supply dewar again. This operation cooled the entire flow system in preparation for a test. The test section and connecting piping were kept full of liquid (at near-ambient pressure) during preparatory and calibration periods between tests; therefore, the plastic venturi was generally colder than the test liquid in the supply dewar when a test was started. Next, the liquid in the supply dewar was heated to the desired temperature. Supply and receiver dewars were then pressurized to appropriate levels, throttle valve D was positioned, and flow started by opening valve C. In the case of non-cavitating flow, inception was induced by further opening valve D and thus increasing the flow velocity until vapor appeared. To obtain desinent cavitation or non-cavitating flow from fully developed cavitating flow, valve D was further closed until the vapor cavity was

barely visible. For developed-cavity tests, valve D was adjusted to obtain the desired cavity length. Flow was terminated by closing valve C. The supply dewar was then vented and the test liquid transferred back into the supply dewar for another test. As previously mentioned, the entire test event was recorded on movie film which was subsequently used to determine incipience, desinence, and desired cavity lengths.

A concrete protective barrier separated operating personnel from the test apparatus, and all tests were remotely controlled. Valve D was electrically driven and the receiver dewar pressure was remotely controlled by means of a pneumatic transmitter, differential controller, and vent valve arrangement, figure 3.1. The supply dewar and valve C were also remotely controlled with pneumatics.

5. DATA ANALYSIS

The developed cavitation data for liquid hydrogen are given in complete detail in appendix A. Typical profiles of measured pressure depression are given on figures 5.1 to 5.5. Photographs of fully developed vaporous cavities in liquid hydrogen are shown on figure 5.6. Inlet velocity and temperature were observed to have very little effect on the appearance of cavitating hydrogen; i.e., the cavities were generally well defined and uniformly developed.

5.1 Metastable Trends in Vaporous Hydrogen Cavities

In figures 5.1 to 5.5, the data points representing cavity pressure measurements have been connected with a smooth curve to facilitate comparison with the data points obtained from the cavity temperature measurements. The pressure depressions obtained from the cavity temperature measurements are, for the most part, greater than those derived from the measured cavity pressures. The new hydrogen data indicate that the cavity pressures and temperatures are nearly in

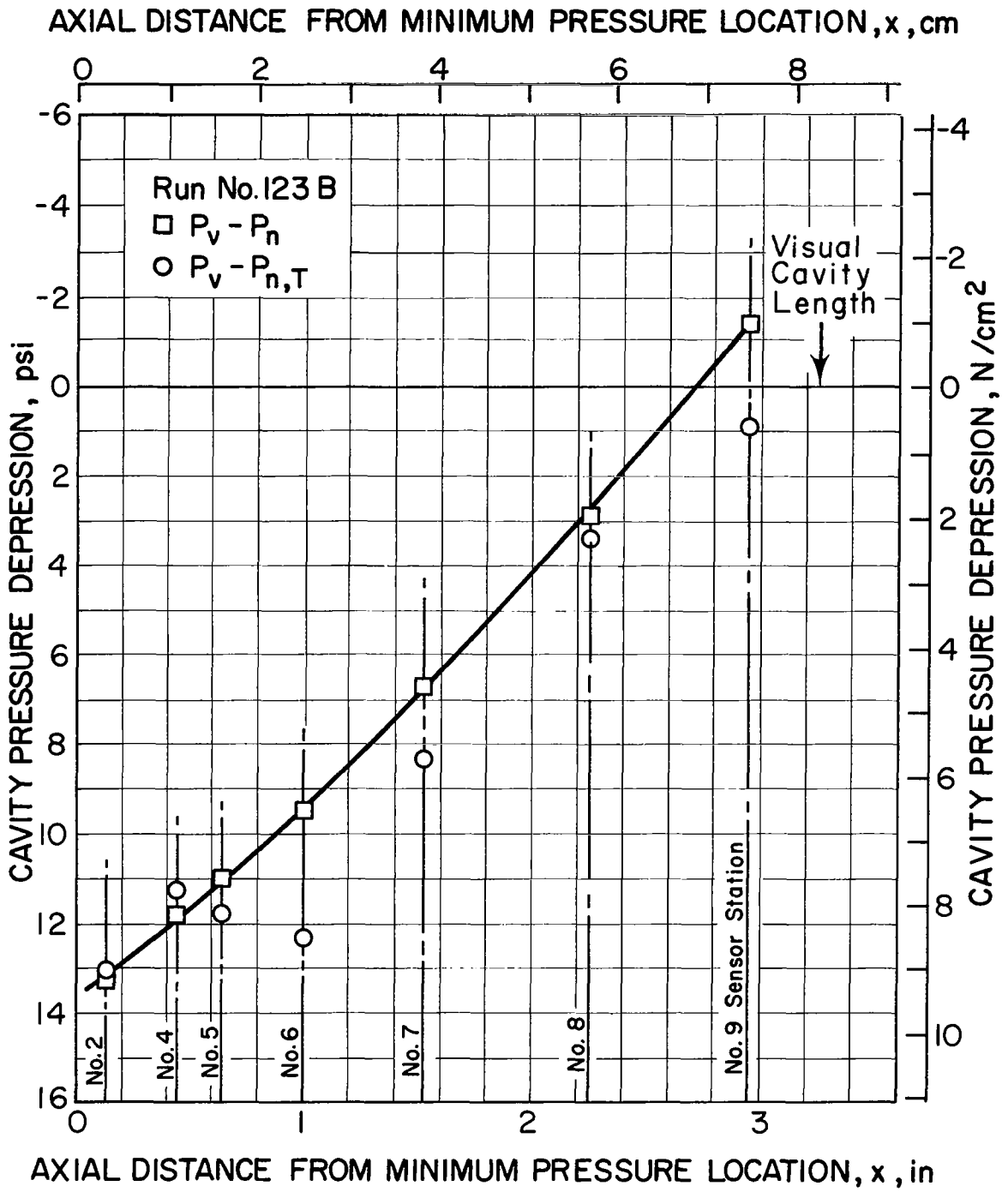

Figure 5.1 Pressure and temperature depressions within cavity in liquid hydrogen.

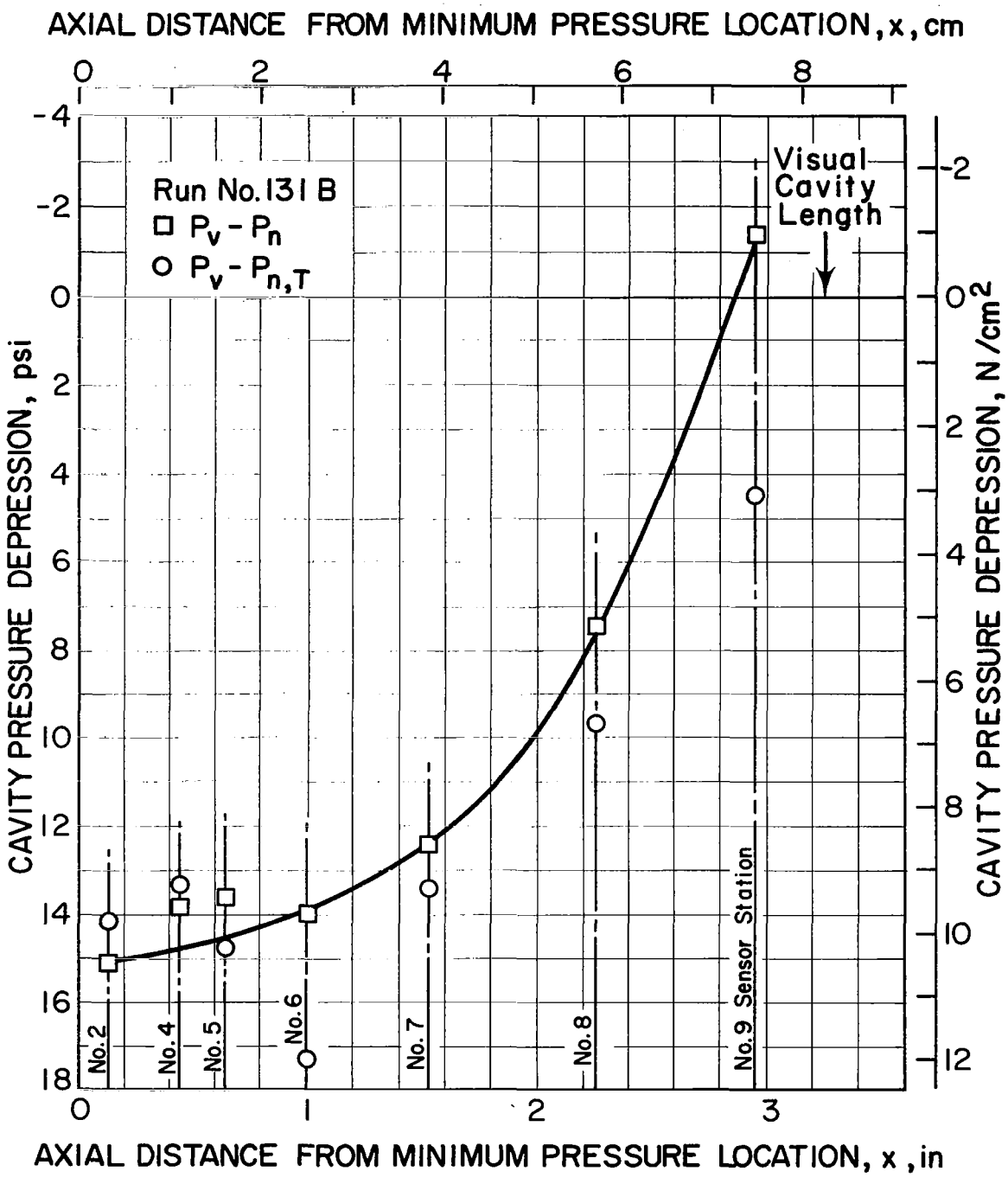

Figure 5.2 Pressure and temperature depressions within cavity in liquid hydrogen.

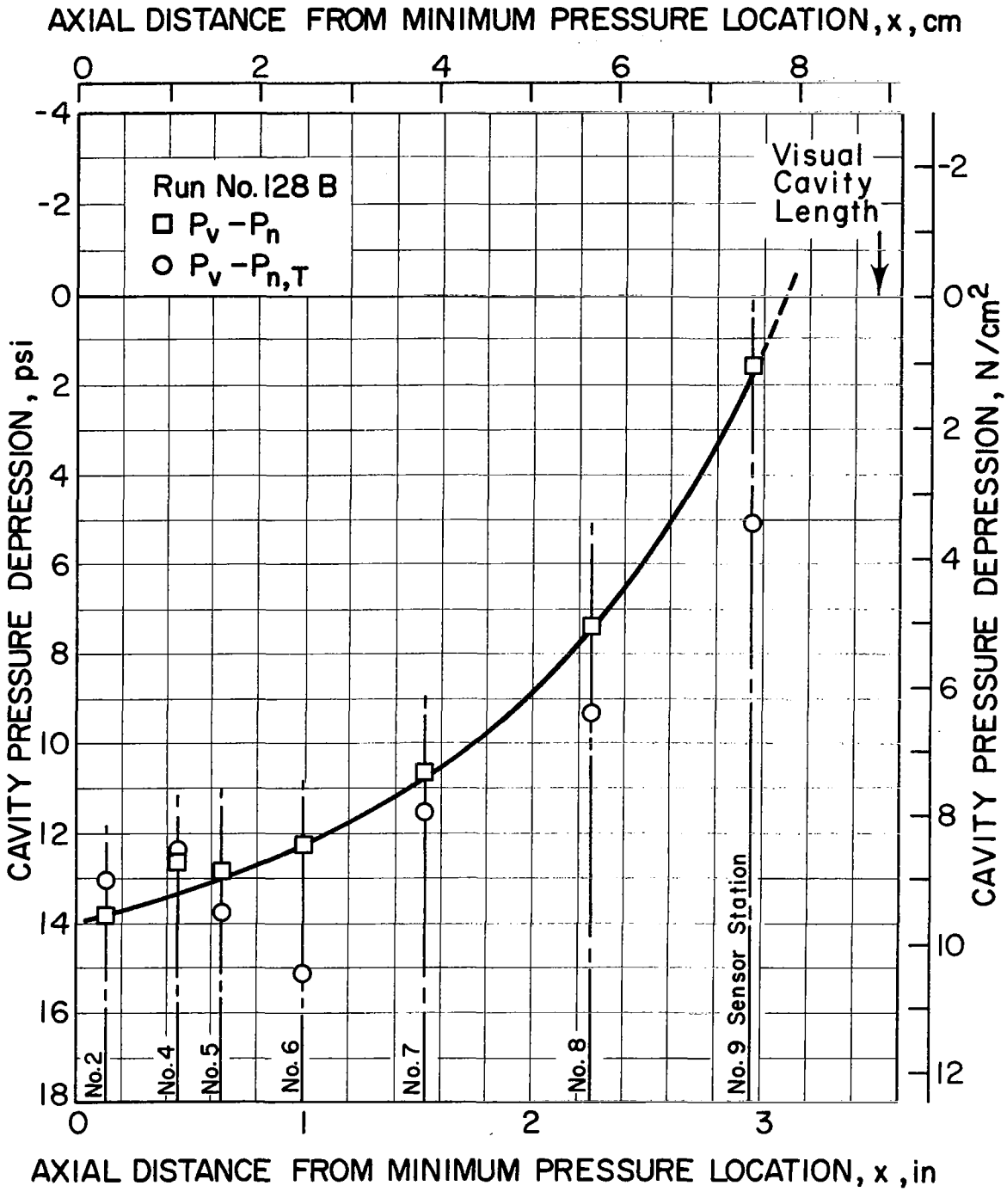

Figure 5.3 Pressure and temperature depressions within cavity in liquid hydrogen.

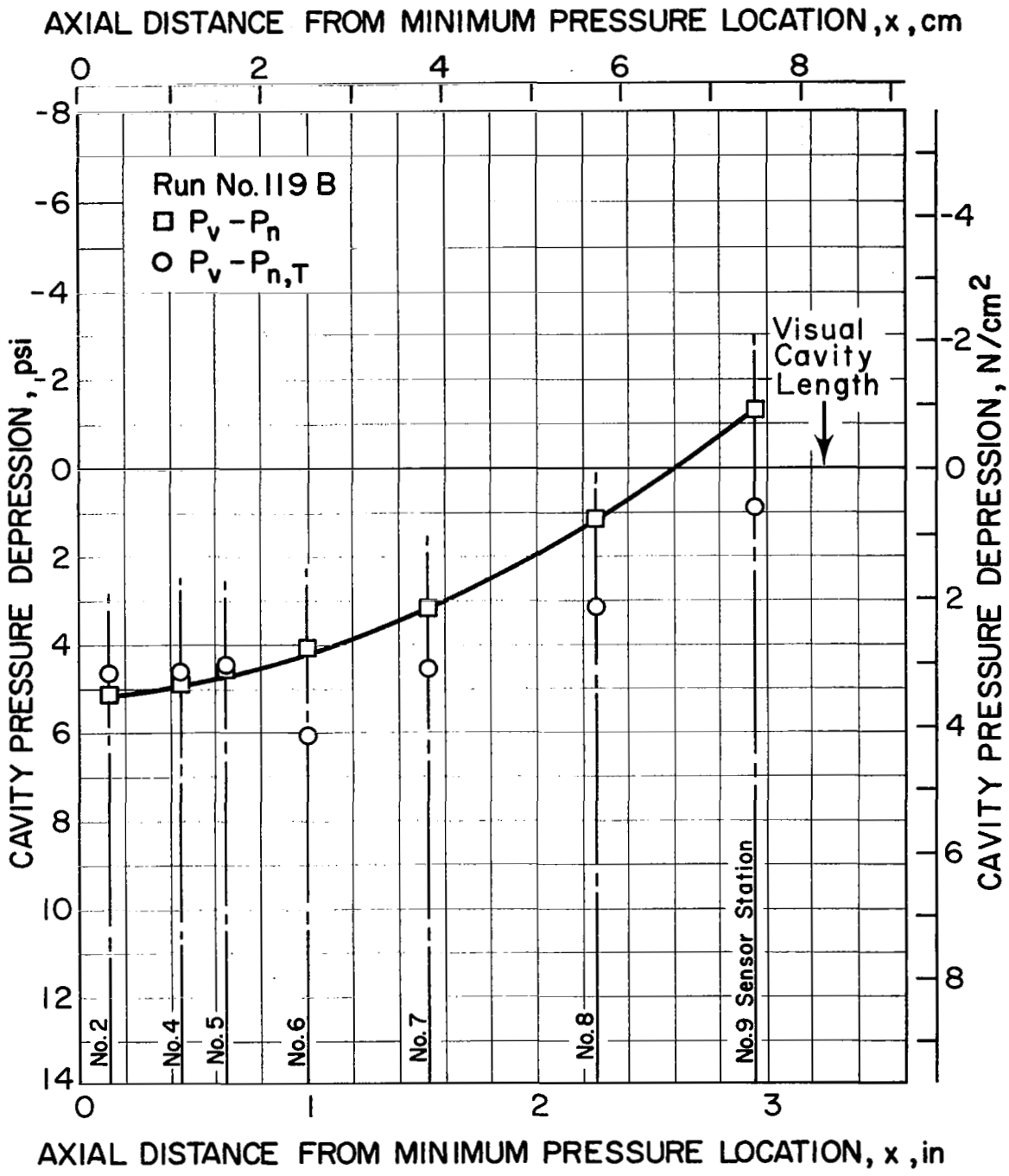

Figure 5.4 Pressure and temperature depressions within cavity in liquid hydrogen.

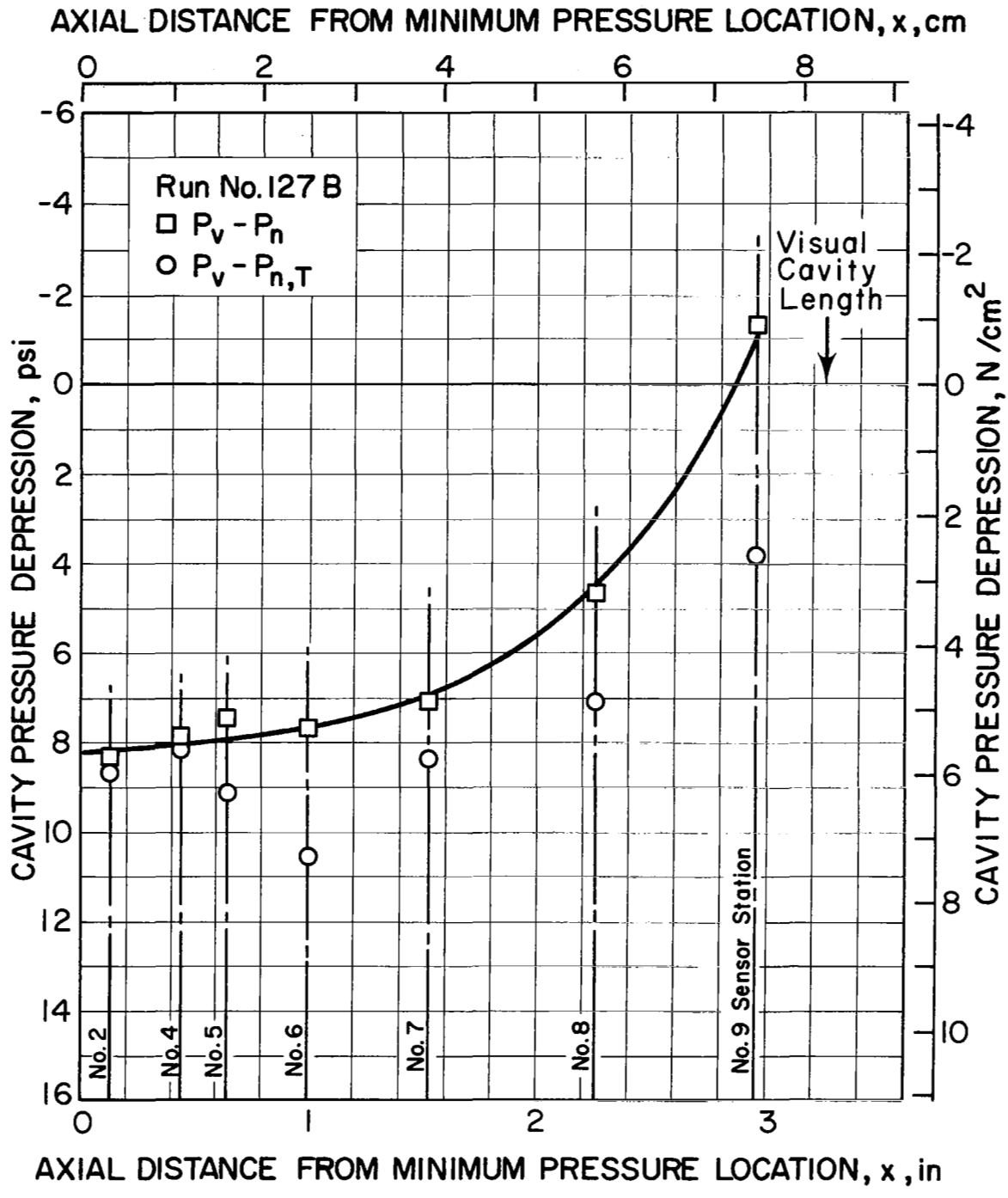

Figure 5.5 Pressure and temperature depressions within cavity in liquid hydrogen.

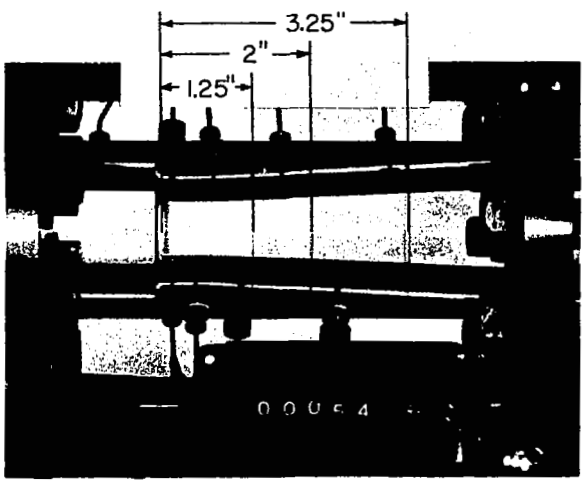

(.1): Typical incipient cavitation. Note scribe marks used to identify nominal cavity length.

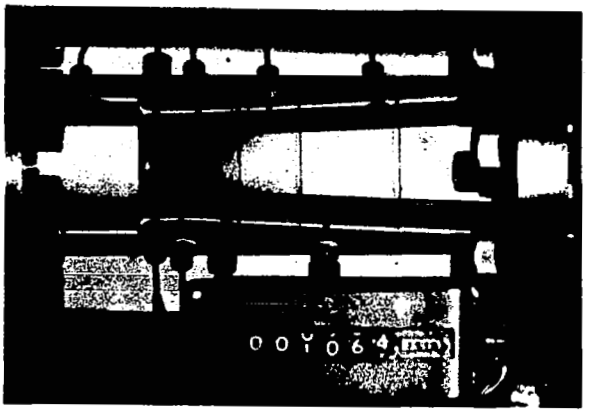

(.2): Nominal cavity length, 1.25-inch (3.2 cm); V_o = 33.8 m/s, T_o = 20.3 K. P_o = 16.1 N/cm^2, K_v = 1.46.

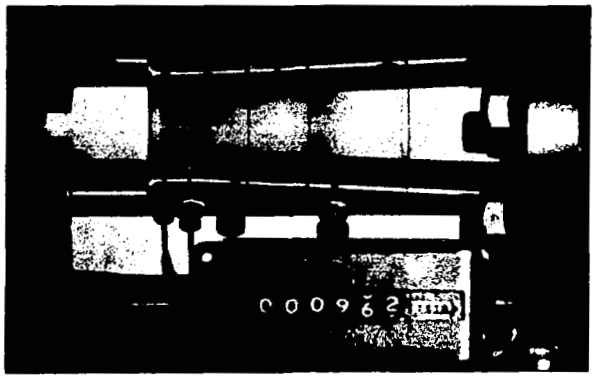

(.3): Nominal cavity length, 2-inch (5.1 cm); V_o = 47.2 m/s, T_o = 20.4 K, P_o = 25.1 N/cm^2, K_v = 1.83.

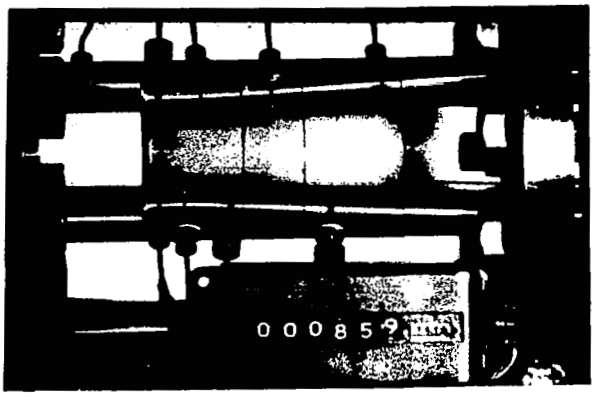

(.4): Nominal cavity length, 3.25-inch (8.25 cm); V_o = 62.5 m/s, T_o = 22.7 K, P_o = 41.0 N/cm^2, K_v = 1.60.

Figure 5.6 Photographs showing typical appearance of developed cavities in liquid hydrogen.

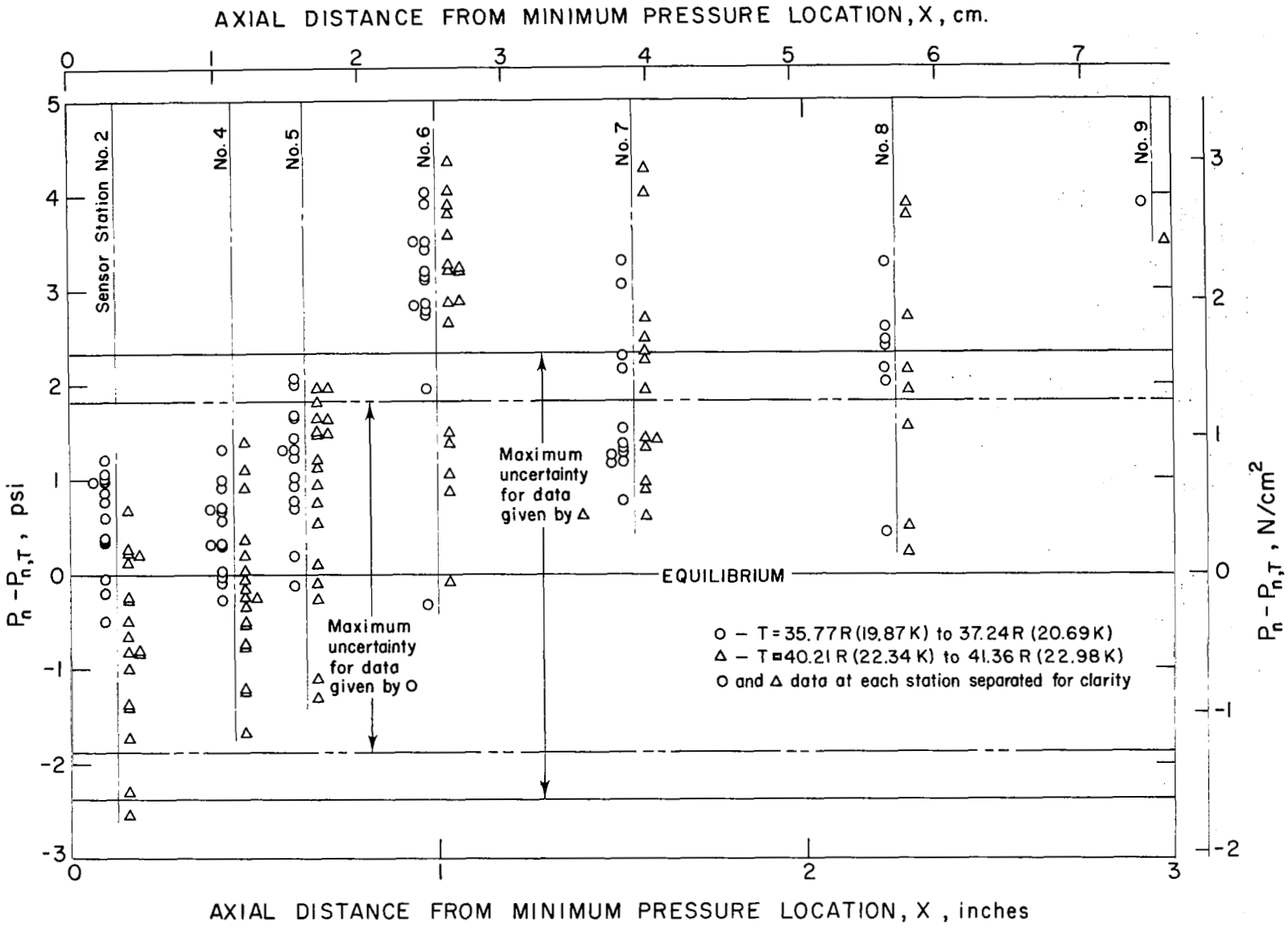

Figure 5.7 Characteristics of thermodynamic metastability in vaporous hydrogen cavities.

thermodynamic equilibrium near the leading edge of the cavity where vaporization occurs; these data also substantiate metastability in the central and aft regions of the vaporous hydrogen cavities. This is an important observation, because it was shown in reference [20] that the B-factor theory requires only that thermodynamic equilibrium prevail during the vaporization process; consequently, only the leading edge of the developed cavity must be in thermodynamic equilibrium. The central and trailing regions of the cavity, where condensation occurs, apparently are not in stable thermodynamic equilibrium.

The magnitude of thermodynamic metastability within the hydrogen cavities is plotted, for all of the new data, on figure 5.7. The maximum overall uncertainty in the data is clearly indicated on figure 5.7; this maximum uncertainty is obtained by the simple addition of the overall uncertainties in P_n and $P_{n,T}$. From section 3.2 of this paper, the estimated overall uncertainty in P_n is ± 1.0 psi (± 0.69 N/cm^2) and the uncertainty in T_n is ± 0.36 R (± 0.20 K). Converting the uncertainty in T_n into uncertainty in $P_{n,T}$ merely requires evaluation of the slope of the saturation liquid-vapor pressure-temperature equilibrium curve at the appropriate T_n. The product of this slope and the uncertainty in T_n is the estimated uncertainty in $P_{n,T}$. Because the uncertainty in $P_{n,T}$ varies with temperature level, the data have been separated on figure 5.7 into two discrete groups; each group identifies with a prescribed fluid temperature bandwidth and the associated maximum uncertainty in the data. The estimated overall uncertainty in $P_{n,T}$ at the lower temperature level is (2.39 psi/R)x 0.36 R = 0.86 psi (0.59 N/cm^2), and at the higher temperature level is (3.75 psi/R)x 0.36R = 1.35 psi (0.93 N/cm^2). Errors in the hydrogen property data will be taken as negligible in this analysis. The uncertainty bands indicated on figures 5.7 are obtained by adding 1.0 psi (0.69 N/cm^2) to the uncertainties in $P_{n,T}$ listed above. These limits appear quite realistic as they encompass

practically all of the data at instrument stations 2 and 4, where equilibrium apparently exists; the distribution of data points at these two stations lends credence to this statement. Stations 6 to 9 exhibit a definite trend toward metastable vapor, with the maximum consistent metastability occurring near station 6.

These results confirm the initial work [16] where cavity temperatures were measured at stations 2, 6, and 8 only. It is felt that the data plotted on figure 5.7 is positive evidence that metastable vapor exists in the central and aft regions of the hydrogen cavities. In this plot, no attempt was made to separate the effects of velocity and cavity length; considerably more data would probably be required, and such effort does not appear warranted at this time. From figure 5.7, it appears that fluid temperature does not have a significant effect on the magnitude of $P_n - P_{n,T}$.

From figure 5.7, it can be observed that, within data accuracy, thermodynamic equilibrium exists in the frontal regions of the cavity. Over the remaining cavity length, it appears that condensation occurs--an important consideration for future modeling theories. Because of the importance of this result, one is tempted to hypothesize an explanation for the results shown on figure 5.7. Accordingly, the following discussion should be considered as conjectural.

5.2 Simplified Analysis of Metastable Phenomena

Flow patterns, circulation, turbulence, and vapor velocity within the cavities are unknown; consequently, it is difficult--if not impossible--to perform a thermodynamic fluid flow analysis on the liquid-vapor exchange. Thus, we shall limit our discussion to a highly simplified analysis in order to obtain some crude explanatory results. We will assume that the developed cavity can be represented by an agglomeration

of single spherical bubbles moving with the bulkstream liquid; we can then use the existing solutions [21] for bubble dynamics. These solutions are available in simplified form, appropriate for the approximate solutions we seek.

The following assumptions were used to obtain the simplified expressions for vapor-filled bubbles: The flow is taken as steady and irrotational; compressibility of the liquid, heat flow, viscosity and surface tension effects are neglected. Also, a constant pressure and temperature in the bulkstream liquid is assumed. Inertial forces are considered dominant, and thermal boundary conditions and pressure fluctuations are ignored; for our problem, this constitutes the only serious breach between the simplifying assumptions and our intended application. We know that heat transfer and pressure gradients play an important role in the formation and sustenance of a developed vapor cavity. A more rigorous solution, including pressure variations and heat transfer to a single bubble, is a complex task [22] and for the purpose of this discussion is not warranted; particularly, since our problem involves an annular developed vapor cavity. In simplified form, the cavity growth rate approaches the value given by

$$\dot{R}_G \approx 0.82 \left[\frac{P_{n,T} - P_n}{\rho_o} \right]^{0.5} \qquad (5.2\text{-}1)$$

and the collapse rate is approximated by

$$\dot{R}_C \approx 0.82 \left[\frac{P_n - P_{n,T}}{\rho_o} \right]^{0.5} \left[\left(\frac{R_i}{R} \right)^3 - 1 \right]^{0.5} . \qquad (5.2\text{-}2)$$

The pressure differences used to calculate cavity growth and collapse rates in the foregoing equations have been chosen to take advantage of measurements provided by this study. Also, extension of the spherical bubble formulae [21] to our annular cavity problem requires some improvisation. The conventional bubble formulae [21] use $P_{v,x} - P_{\ell,x}$ in eq (5.2-1) and $P_{\ell,x} - P_{v,x}$ in eq (5.2-2). That we cannot blindly use these quantities is apparent because 1) $P_{\ell,x}$ is unknown--it is not measured and is difficult to calculate because it varies continuously with cavity length and is also influenced by the unknown cavity thickness, 2) $P_{v,x}$ is not constant--it varies continuously along the annular cavity interface as a result of vaporization (or condensation) and changing bulkstream liquid pressure. Extrapolation of the bubble formulae to the annular cavity may be accomplished by assuming 1) that the liquid pressure, $P_{\ell,x}$, is adequately approximated by P_n and 2) that the local vapor pressure, $P_{v,x}$, can be represented by $P_{n,T}$. Subsequently, we shall see that $P_{n,T}$ ($\approx P_{v,x}$) cannot differ appreciably from P_v at (or near) the leading edge of the annular cavity. Then the pressure difference, $P_{n,T} - P_n$, is the driving potential for vaporization, and $P_n - P_{n,T}$ causes condensation to occur.

To graphically illustrate the foregoing discussion, we compare pertinent pressure profiles on figure 5.8. This plot shows the venturi pressure distributions for non-cavitating flow (P_x) and cavitating flow (P_n and $P_{n,T}$); the venturi inlet liquid bulkstream vapor pressure, P_v, is also shown. All of these data are considered typical and were obtained from Run 123B, as tabulated in appendix A. The data plotted on figure 5.1 can be obtained directly from the information shown on figure 5.8. P_x, on figure 5.8, was computed by combining the test data for Run 123B with the pressure coefficient data given on figure 3.5.

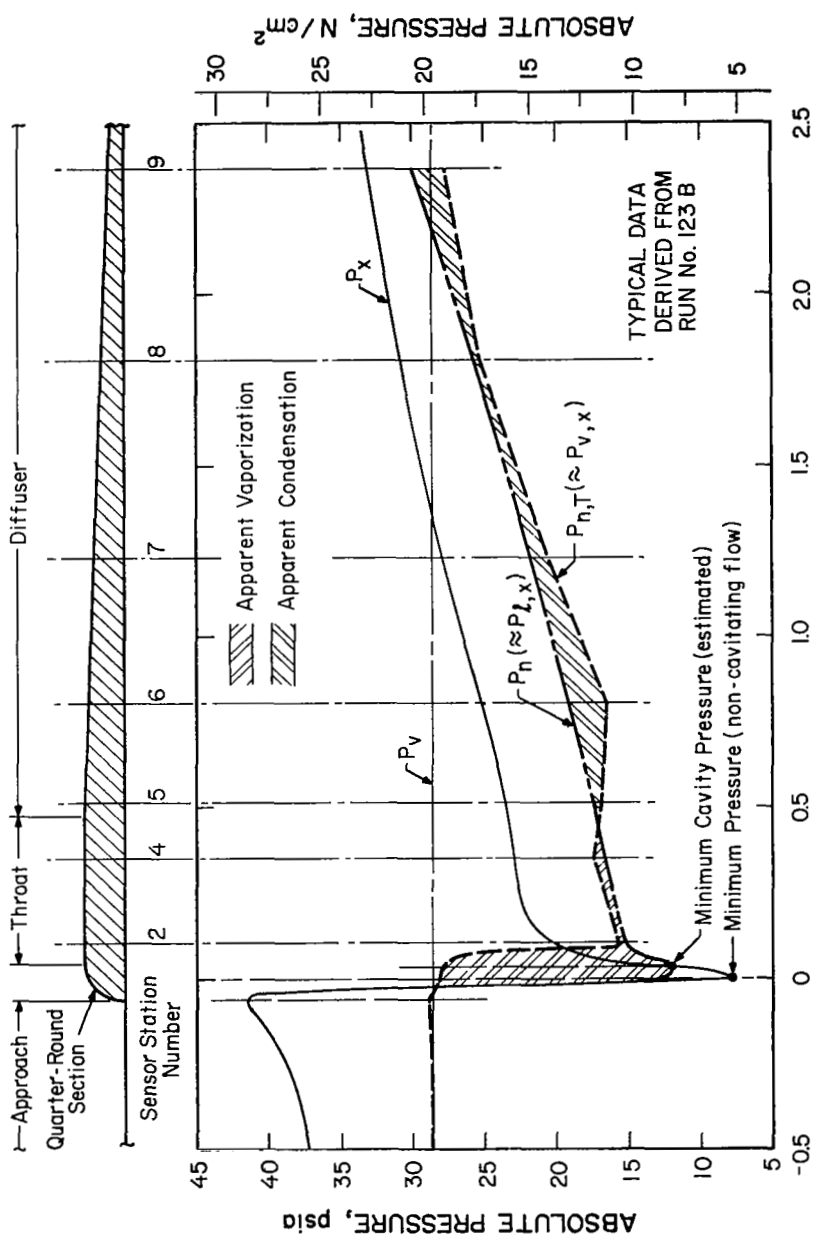

Figure 5.8 Typical pressure distribution through test section for cavitating and non-cavitating flow.

P_n and $P_{n,T}$, on figure 5.8, were plotted directly from test data for stations 2 through 9; upstream of station 2, P_n and $P_{n,T}$ were estimated. The shape of the P_n curve upstream of station 2 is in agreement with the generalized results of Rouse and McNown [25]; i.e., for various cavitating bodies [25], as cavitation progresses, the minimum pressure increases while shifting slightly downstream and forming a shallower, but wider pressure 'trough'. The P_n and P_x curves are coincident just upstream of the minimum pressure point. The shape of the $P_{n,T}$ curve upstream of station 2 is compatible with visual and photographic observations from this study and previous work [15]. These visual data indicate that the leading edge of the cavity always originates near, or slightly downstream of the non-cavitating minimum pressure point. If we select the cavitating minimum pressure point as the leading edge of the cavity, we may construct the $P_{n,T}$ ($\approx P_{v,x}$) curve upstream of station 2 as follows: 1) the local vapor pressure, $P_{n,T}$, is coincident with P_v in the venturi inlet, 2) $P_{n,T}$ increases slightly at the stagnation point on the quarter-round contour due to the increase in P_n (or P_x), 3) $P_{n,T}$ decreases as P_n decreases to a minimal value and 4) $P_{n,T}$ decreases rapidly, as a result of vaporization, to the measured value of $P_{2,T}$. The shaded regions between the P_n and $P_{n,T}$ curves on figure 5.8 indicate where apparent vaporization and condensation occur. The shaded region upstream of station 2 indicates that $P_v - P_n$ should provide adequate estimates for cavity growth in this area. From figure 5.7, we recall that apparent thermodynamic equilibrium generally exists at stations 2 and 4. Then little or no growth would be expected in this vicinity, see figure 5.8; however, from physical considerations, the cavity thickness must increase between stations 2 and 4 in the venturi throat. All cavitating bodies [25] show cavity thickness increasing

with increasing cavity length in the front portion of the cavity. Although the instrumentation is not sufficiently precise to indicate the exact magnitude of $P_{n,T} - P_n$, it is apparent that some additional vaporization must occur in this region to support the increased cavity thickness. The measured values of P_n and $P_{n,T}$, as shown on figures 5.1 to 5.5, 5.7, and 5.8, imply that only slight vaporization can occur between stations 2 and 5. The above mentioned figures also indicate that transition from vaporization to condensation generally occurs between stations 4 and 6 and commonly occurs between stations 4 and 5. Then, from this discussion we may conclude that vaporization normally prevails upstream of station 5 and condensation occurs downstream of this location.

It is interesting to note that station 5 coincides closely with the venturi throat-to-diffuser transition, see figure 5.8. Since the diffuser was designed to provide efficient liquid pressure recovery, a condition favoring condensation, it is reasonable that condensation should commence near station 5. It appears that our data, e.g., see figure 5.8, are in good agreement with physical considerations.

To avoid confusion, we emphasize that: 1) $P_{n,T}$ ($\approx P_{v,x}$) differs appreciably from P_v at all cavity locations downstream of station 2, see figure 5.8, 2) use of $P_v - P_n$ in eq (5.2-1) is valid only at locations upstream of station 2 and therefore 3) positive values of $P_v - P_n$ downstream of station 2 do not predict that vaporization should extend over the entire length of the cavity. Likewise, it should not be erroneously concluded from inspection of eq (5.2-2) that the cavity will not collapse unless P_n exceeds $P_{n,T}$. Measured values of P_n and $P_{n,T}$ were chosen to approximate $P_{\ell,x}$ and $P_{v,x}$, respectively. The actual position of the $P_{\ell,x}$ and $P_{v,x}$ profiles on figure 5.8 are unknown; therefore the unknown quantity $P_{\ell,x} - P_{v,x}$ can dictate cavity collapse, even though the cavity vapor is in apparent thermodynamic equilibrium, i.e., $P_n = P_{n,T}$.

In summary, formulae applicable to spherical bubbles are being used to estimate vaporization and condensation rates at specific locations within an annular cavity; the bubble formulae apply to a uniform pressure and temperature field (liquid), but the annular cavity is immersed in a nonuniform pressure and temperature field. Pressure and temperature data from this study are used in conjunction with these formulae to perform computations at fixed points within the annular cavity. In this way, the simplified formulae are adapted to our complex problem (where heat transfer and pressure variations prevail).

The cavity growth rate is bounded by eq (5.2-1), but the collapse rate increases without bound as the cavity collapse progresses. Careful study of eq (5.2-2) indicates that $\dot{R}_C$ increases almost linearly with decreasing R until $R \approx R_i/2$; thereafter, $\dot{R}_C$ increases according to the $R^{-3/2}$ relationship. Therefore, it can be shown that the additional time required for completion of cavity collapse after $R = R_i/4$ is negligible. More than 97 percent of the total collapse time is incurred in reducing the bubble radius to $R_i/4$. We may then obtain a characteristic collapse rate by integrating eq (5.2-2) over the radius interval, $R_i/4$ to R_i, and calculating the mean collapse rate, $\overline{\dot{R}}_C$:

$$\overline{\dot{R}}_C \approx 2 \left\{ \frac{P_n - P_{n,T}}{\rho_o} \right\}^{0.5} . \qquad (5.2\text{-}3)$$

The ratio of apparent collapse/growth rates may then be written as

$$\overline{\dot{R}}_C / \dot{R}_G \approx 2.5 \left\{ \frac{P_n - P_{n,T}}{P_{n,T} - P_n} \right\}^{0.5} . \qquad (5.2\text{-}4)$$

So, for equal vapor and liquid metastabilities, i.e., $P_n - P_{n,T} = P_{n,T} - P_n$, a bubble will collapse 2.5 times as fast as it will grow. In our experiments, $P_{n,T} - P_n$ at the leading edge of the cavity far exceeds $P_n - P_{n,T}$ in the middle and aft regions of the cavity. Simultaneous inspection of eq (5.2-4) and figure 5.8 indicates that $\bar{\dot{R}}_C/\dot{R}_G$ can vary widely with the values selected for $P_n - P_{n,T}$ and $P_{n,T} - P_n$. For the purpose of this discussion, we simply need the <u>average</u> values of these pressure differences on either side of station 5. We can then compare, on the average, the growth rate upstream of station 5 to the collapse rate downstream of station 5. Referring to figure 5.8, and using the data tabulated in appendix A, we obtain for these average values, $P_{n,T} - P_n \approx 3.8$ psi (2.6 N/cm^2) and $P_n - P_{n,T} \approx 1.5$ psi (1.04 N/cm^2). Data uncertainty and data near the irregular, trailing edges of the cavity (station 9) are neglected in this estimate; actually, station 9 data may be included with little effect on the computations performed herein. Applying these mean values of pressure-difference to eq (5.2-4), we obtain $\bar{\dot{R}}_C/\dot{R}_G \approx 1.6$, i.e., the growth time exceeds the collapse time by about 60 percent. Applying this same approach to figures 5.2 through 5.5, we find that $\bar{\dot{R}}_C/\dot{R}_G$ varies from about 1.5 to 2.5.

Within the bounds of this rough computation, we may then conclude that the growth and collapse rates are not much different. For constant liquid velocity in the cavitated region, this implies that vaporization and condensation should occupy about the same fraction of cavity length. Referring to figure 5.8, we see that the axial distance from the minimum pressure point to station 5 is about half the distance between stations 6 and 8 and about one-third the distance between stations 6 and 9. For shorter cavities, this distance ratio will approach

unity and our computations will agree more closely with the test data. Because of the assumptions and approximations involved, the analysis presented here is highly simplified, but it certainly does not detract from the results shown on figure 5.7. It seems totally plausible that metastable vapor should exist in the downstream regions of the cavity.

To conclude this conjectural discussion, we must estimate the liquid velocity at the liquid-vapor interface. We will assume that the area available for liquid flow in the cavitated region is constant and is equivalent to the venturi throat area. For the experiments reported here, the liquid velocities in the throat varied from about 150 to 300 ft/s (45.7 to 91.5 m/s)--these velocities were undoubtedly higher due to the presence of the annular cavity of unknown thickness. The time required for a particle of liquid to traverse the liquid-vapor interface of the longest cavity is then computed by dividing the cavity length by the velocities given above; 0.8 to 1.6 milliseconds transit time is required. This transit time is shorter for higher liquid velocities and shorter cavities. Obviously, little time is available for vaporization and condensation to take place, and the metastable behavior depicted on figure 5.7 is not too surprising.

Actually, the thermal-response of the liquid, to rapidly varying pressure, as a particle of liquid traverses the venturi contour will determine where vaporization effectively stops and condensation starts. The transition from vaporization to condensation will occur at slightly different locations within the cavity as the fluid temperature, velocity, cavity length, etc., are varied. An analytical model, with appropriate provisions for heat transfer and time-dependent pressure, is required to shed more light on this topic; at this point, we conclude our conjecture.

With respect to the foregoing analysis, we note that the liquid velocities in the vicinity of the cavities exceed the two-phase sonic velocity for hydrogen. We should also note that on occasion we have observed, on film, apparent "shock waves" traveling back and forth within the cavitated regions. These "shocks" manifest themselves as sharply-contrasted density discontinuities, made visible by the accompanying variation in refractive index.

5.3 Data Correlation

The correlative technique developed by Gelder, et al. [15], was used to correlate the data from this experiment. This technique has proven highly successful and is an extension of the B-factor[2] concept. A brief history on the development of the B-factor concept and a simplified and improved method for computing B-factor were recently published [20]. Although the current B-factor approach is not entirely compatible with the physical processes of cavitation, it is well established, adequately documented, and provides good results [4, 5]. Recent efforts [23] to obtain a more compatible theory have not yet resulted in a predictive technique that is less complex or less dependent upon experimental data. The basic correlation expression is based upon dynamically and geometrically similar cavities. Thus, for convenience, we will frequently refer to this correlative expression as the 'similarity' equation. The similarity equation is used to correlate developed-cavitation data in similar test items and to predict the cavitating performance of a test item from fluid-to-fluid and from one temperature to another, when limited data from a single fluid are

---

[2] B is defined as the ratio of the volume of vapor to the volume of liquid involved in sustaining a developed vaporous cavity.

available. The similarity equation in its final form is given [3] as

$$B = (B)_{ref} \left(\frac{\alpha_{ref}}{\alpha} \right)^{E1} \left(\frac{V_o}{V_{o,ref}} \right)^{E2} \left(\frac{\ell}{\ell_{ref}} \right)^{E3} \left(\frac{D_o}{D_{o,ref}} \right)^{E4} ; \qquad (5.3\text{-}1)$$

the symbols are identified in the nomenclature of this paper. To account for differences in theory and experiment, the exponents on the various terms in eq (5.3-1) are individually evaluated using the experimental data and theoretical data [20] for B as follows:

(1) A theoretical value of B is obtained for each experimental data point using the measured cavity pressure-depression $(P_v - P_2)$, T_o, and the calculation method outlined in reference [20]. This value of B is derived under the assumption that the vaporous cavity is formed by the isentropic vaporization of liquid and is referred to herein as B_t.

(2) One experimental data point is arbitrarily chosen as a "reference"; the α, V_o, ℓ, D_o, and B_t from the chosen test are then inserted into eq (5.3-1) as constants where the subscript "ref" occurs. As explained in appendix C, a reference data point is ultimately chosen as that run which provides the best solution to eq (5.3-1) and is therefore most representative of all data being correlated.

(3) Values of α, V_o, ℓ, and D_o from each data point are then inserted into eq (5.3-1) as the non-subscripted terms. This produces an equation for every data point except the one chosen as a reference. Note that the unknowns in the set of simultaneous equations are B and the exponents E1, E2, E3, and E4.

(4) The digital computer is then programmed--see appendix C--to determine the values of E1, E2, E3, and E4 that provide the

best agreement between the computed B (left side of eq (5. 3-1)) and the theoretical B_t obtained in step (1) for all data points considered. The least squares technique used to evaluate these exponents is by no means trivial and is treated with appropriate detail in appendix C. This method ensures that the calculated B values and the B_t values for each data point are as nearly identical as possible; the exponents computed in this manner represent the best possible agreement between experiment, eq (5. 3-1), and the isentropic flashing theory. Recall that the theoretical B_t (step 1) and the calculated B (eq (5. 3-1)) both rely on experimental data at each data point.

The approach outlined above is applicable to any number of terms in eq (5. 3-1). As shown in the computer programs listed in appendix C, two additional terms were provided. Kinematic viscosity was included as a correlating parameter, because it has shown promise in some recent studies [23]; also, modification of the Gelder, et al. [15], theory to account for convection introduces the viscosity term. A surface tension term was also tried,because this fluid property has long been recognized [24] as a candidate correlating parameter and because the Weber number is vital to dynamic similitude studies involving the formation of bubbles, break-up of liquid jets, etc. Both of these fluid properties could justifiably be introduced through a dimensionless analysis approach; viscosity entering through the Prandtl or Reynolds numbers and surface tension by the Weber number.

In eq (5. 3-1), the fluid physical properties are evaluated at P_o and T_o and the standard deviation in B is computed for each set of exponents; the individual exponents may be held constant or chosen by the computer. The standard deviation in B factor is minimized in the

computer programs when one or more of the exponents is selected by the computer; the absolute minimum standard deviation is obtained when all of the exponents are selected by the computer. The standard deviation is simply computed in those cases where the exponents are held constant. The set of exponents that produces minimum standard deviation in B is selected as the best correlative solution for any particular batch of data; i. e. , the standard deviation is a measure of the validity of the similarity and isentropic-flashing theories, as both are evaluated from experimental data. Data from the initial study [16] and the new data were separately and collectively correlated using the approach described herein. The results of this effort are given in table 5. 1, along with the results of others [3], and are discussed in the following section of this paper.

5. 4 Discussion of Correlative Results and Data

The similarity equation, used to correlate cavitation performance of a particular flow device from fluid-to-fluid, was fitted with numerical exponents derived from the experimental data of this study. The similarity equation and exponent data for hydrogen-refrigerant 114 were obtained from the literature; the numerical exponents for hydrogen-refrigerant 114 are compared in table 5. 1 with those deduced from this experiment and the initial study [16]. The exponents given in table 5. 1 were obtained with a least-squares fitting technique and a digital computer; the suitability of the various exponents to the experimental data is indicated by the standard deviation in B-factor as explained previously. In this study, the value of B ranges from two to five.

As indicated in table 5. 1, there is little difference in the exponents obtained from the old data (line 1), new data (line 2), and combined old and new data (line 3); also, the data of Moore and Ruggeri [3] for

Table 5.1: Correlation of liquid hydrogen data using the 'similarity' equation.

Fluids	Source of Data	Reference Run No.	Exponents ‡			Standard † Deviation in B-Factor	$\overline{K}_c$, min
			E1	E2	E3		
H_2	Reference [16]	071C	-1.94	0.71	0.31	0.3457	2.445
H_2	This Study	128B	-1.62	0.78	0.34	0.3553	2.473
H_2	This Study + Ref [16]	071C	-1.92	0.74	0.31	0.3466	2.459
H_2 & F-114	Reference [3]	- - -	1.0	0.8	0.3	- - - -	2.47

‡ $$B = B_{ref}\left(\frac{\alpha_{ref}}{\alpha}\right)^{E1}\left(\frac{V_o}{V_{o,ref}}\right)^{E2}\left(\frac{\ell}{\ell_{ref}}\right)^{E3}$$

† Standard Deviation $\equiv \sqrt{\left[\sum(B-B_t)^2\right]/(NPTS-1)}$, where NPTS = number of data points (including "ref" data point), B_t is computed from isentropic-flashing theory [20], and B is computed from eq (5.3-1).

hydrogen-refrigerant 114 is in reasonable agreement, excluding the diffusivity term. The lack of variation in α (< 10 percent) explains why E1 tends to a negative number when correlating with liquid hydrogen alone. Gelder, et al. [15], obtained a value of 0.5 for E1 when correlating refrigerant 114 data with 25 percent variation in α. There was over 400 percent change in α in the hydrogen-refrigerant 114 data correlated by Moore and Ruggeri [3], and thus the value for E1 reported in line 4 of table 5.1 is to be preferred. The mathematical technique used to derive the exponents can easily pick an extraneous value for any of the exponents if there does not exist significant variation in the corresponding physical parameter.

Introduction of the viscosity and surface tension terms into eq (5.3-1) did not significantly improve the hydrogen data correlation, and consequently exponents for these terms are not included in table 5.1; however, these terms may be important correlating parameters when attempting to correlate data from fluid-to-fluid. It is anticipated that both of these parameters may improve data correlation where sufficient variation in the fluid properties occurs. In the hydrogen data of this study, the viscosity varied less than 20 percent and the surface tension varied less than 40 percent. Correlation of the hydrogen-refrigerant 114 data would most likely be improved by using one or both of these terms.

The diameter term in eq (5.3-1) was not included in table 5.1, because our tests were conducted with only one venturi size. Moore and Ruggeri [3] obtained an exponent value of -0.1 for the diameter term, based on tests using refrigerant 114 in two different venturi sizes. Those tests were performed with a venturi identical to the one used in this study and with a larger (1.414:1) geometrically similar venturi.

The arithmetic mean[3] value of the developed cavitation parameter, $\overline{K}_{c,min}$, does not vary appreciably for all data considered in table 5.1; this is an important result, and constant $\overline{K}_{c,min}$, eq (5.3-1), and the isentropic-flashing theory are used to predict [4, 5] the cavitating performance of equipment. It is anticipated that nature will triumph and $\overline{K}_{c,min}$ for other cavitating models will not remain constant for all fluids, cavity lengths, velocities, temperatures, etc. $\overline{K}_{c,min}$, of course, varies widely with model or equipment geometry, as does the pressure coefficient, C_p. Also, the conventional cavitation parameter for developed cavitation, K_v, varies with flow conditions for any particular geometry, e.g., see table A-1a and Rouse and McNown [25].

The experimentally-determined exponents in eq (5.3-1)--as listed in table 5.1--are based upon pressures measured within the cavity, near the leading edge where equilibrium prevailed in all fluids tested to date. It is clear that the experimental conditions under which the exponents were determined are compatible with the isentropic-flashing theory and local equilibrium throughout the cavitated region is not required. Also, it appears plausible that exponents derived in this manner could easily mask the effects of slight metastabilities (or perhaps unstable equilibria) within vaporous cavities.

The data given on figures 5.1 to 5.5 indicate[4] that some of the cavities were shorter than their visual (as observed on film) length.

---

[3] $K_{c,min}$ for every hydrogen data point was within 7 percent of $\overline{K}_{c,min}$ (excluding Run No. 117).

[4] The pressure-depression should be near zero at the trailing edge of the cavity and the actual length of the cavity may be estimated by extrapolating the data to zero pressure-depression.

The actual length of the cavity and the observed length differ because of irregular trailing edges of the cavity and the difficulty in judging the visual length. Both actual and visual cavity lengths were used to correlate the data, and they produced essentially the same results.

The pressure depression in the cavitated region is determined by subtracting the measured cavity pressure, in one case, and the saturation pressure associated with the measured cavity temperature, in the other case, from the vapor pressure of the liquid entering the test section.

In the data reported here, the minimum measured cavity pressure was less than bulkstream vapor pressure by as much as 15.13 psi (10.44 N/cm^2); these pressure-depressions are obtained by subtracting P_2 from P_v in the tabulated data of appendix A.

Cavity pressure-depression increases with increasing cavity length, fluid temperature, and velocity for these tests. These trends are graphically demonstrated in figures 5.1 to 5.5 and in reference [16]. The data in appendix A also readily disclose these trends if we permit only one of the three parameters (ℓ, V_o, and T_o) to vary at a time and note the value of $P_v - P_2$ for two different values of the parameter being varied. As an example, T_o and V_o are relatively constant in Runs 125A and 125B, but the cavity length differs by a factor of three; $P_v - P_2$ for the longer cavity (Run 125B) is about four times the $P_v - P_2$ for the shorter cavity (Run 125A). Similar comparisons may be made for variations in V_o and T_o, or portions of the data may be plotted collectively on single graphs, etc., to demonstrate these trends. Typical plots (14 graphs) are given in reference [16].

Because of its popularity in the pumping machinery field, pressure-head has been included in the data tabulated in appendix A; however, provision of these data does not mean that the authors approve of the

use of pressure-head terms. On the contrary, this practice is to be discouraged [20] in computations related to the cavitation process. Mathematical conversion of pressure to pressure-head merely requires evaluation of the liquid density at the point of measurement; however, selection of the appropriate liquid density can be a bit perplexing. Figures 5.1 to 5.5 indicate that the measured pressures and temperatures at the same axial location, within the cavities, are generally not in stable thermodynamic equilibrium. Also, due to the thermal expansivity of liquid hydrogen, the bulkstream temperature changes appreciably as the liquid flows through the venturi. The following methods were used to calculate pressure-head from the cavity measurements: (1) Head (h_n) was calculated from measured cavity pressure by using the saturation density at the measured pressure. (2) Head ($h_{n,T}$) was calculated from measured cavity temperature by using the saturation density at the measured temperature. Both values of head are given in the tabulated data in appendix A.

The cavitation parameter for fully developed cavitation, K_v, was calculated and tabulated for each run, see appendix A.

6. CONCLUDING REMARKS

Pressure and temperature profiles were measured within fully developed, vaporous hydrogen cavities; the results are given in appendix A and on figure 5.7. In general, the measured pressure and temperature depressions were not in stable thermodynamic equilibrium; the pressure-depressions obtained from the cavity temperature measurements are usually greater than those derived from the measured cavity pressures, see typical plots in figures 5.1 - 5.5. Specifically, the experiments indicate that the cavity vapor is normally in thermodynamic equilibrium near the leading edge of the cavity, while considerable thermodynamic metastability occurs in the central and trailing regions of the cavity. This behavior is attributed to lag in the thermal-response of the liquid, to rapidly varying pressure, as a particle of liquid traverses the test section contour. Also, it is shown by simplified analysis that inertial effects alone could at least partially account for this behavior. This study confirms the metastability phenomena reported earlier [16].

The experimental data from this study and previous work [16], were used to fit a 'similarity' equation with numerical exponents, see table 5.1; favorable comparisons are drawn between the old data [16], new data, and the work of others [3]. This 'similarity' equation, coupled with the isentropic flashing theory [20], has been proven useful in predicting [4, 5] the cavitating performance of liquid pumps from fluid-to-fluid. Introduction of viscosity and surface tension parameters into the 'similarity' equation did not improve the correlation for the hydrogen data; however, it is anticipated that both of these parameters may improve fluid-to-fluid correlations. An attempt should be made to update the refrigerant 114 - hydrogen correlation [3] using these two additional parameters.

Recent advances in low temperature thermocouple thermometry permit more precise, local temperature measurements within vapor-filled cavities; consequently, experimental data are sufficiently reliable to evaluate future modifications in cavitation modeling theory.

7. NOMENCLATURE

B	=	ratio of vapor to liquid volume associated with the sustenance of a fixed cavity in a liquid
BCONV	=	symbol used in computer programs for B (left side of eq (5.3-1))
BFLASH	=	symbol used in computer programs for B_t
B_t	=	B derived from isentropic flashing theory (Ref. [20])
C_p	=	pressure coefficient [$\equiv (h_x - h_o)/(V_o^2/2g_c)$]
C_p^v	=	minimum pressure coefficient [$\equiv (h^v - h_o)/(V_o^2/2g_c)$]
D_o	=	test section inlet diameter
g_c	=	conversion factor in Newton's law of motion (gravitational acceleration)
h_n	=	(n = 2, 4, 5, 6, 7, 8, or 9): head corresponding to cavity pressure, measured at a particular instrument port in wall of plastic venturi

$h_{n,T}$ = (n = 2, 4, 5, 6, 7, 8, or 9): head corresponding to the saturation pressure at the cavity temperature, measured at a particular instrument port in wall of plastic venturi

h_o = test section inlet head corresponding to absolute inlet pressure

h_v = head corresponding to saturation or vapor pressure at the test section inlet temperature

h_x = head corresponding to absolute pressure, measured at wall of plastic venturi at distance x, downstream of the minimum pressure point--for non-cavitating flow

h^v = head corresponding to the minimum absolute pressure on quarter-round contour of plastic venturi, computed from expression for C_p^v

$K_{c,min}$ = developed cavitation parameter, based on minimum measured cavity pressure $[\equiv (P_o - P_2)/(\rho_o V_o^2/2g_c)]$

$\overline{K}_{c,min}$ = arithmetic mean value of $K_{c,min}$ for a set of data points

K_v = developed cavitation parameter $[\equiv (h_o - h_v)/(V_o^2/2g_c)]$

ℓ = visual (observed on film) length of developed cavities

$P_{\ell,x}$ = local bulkstream liquid pressure at distance x along the cavity interface -- variable for the annular cavity, but taken as constant in the development of eq's (5.2-1) and (5.2-2)

P_n = ($n = 2, 4, 5, 6, 7, 8$, or 9): absolute cavity pressure, measured at a particular station or instrument port in wall of plastic venturi-- also used to approximate $P_{\ell,x}$ in section 5.2

$P_{n,T}$ = ($n = 2, 4, 5, 6, 7, 8$, or 9): saturation pressure corresponding to the measured cavity temperature at a particular station or instrument port in wall of plastic venturi--also used to approximate $P_{v,x}$ in section 5.2

P_o = test section absolute inlet pressure

P_v = saturation or vapor pressure at test section inlet temperature

$P_{v,x}$ = local vapor pressure of liquid at distance x along the cavity interface--variable for the annular cavity, but taken as constant in the development of eq's (5.2-1) and (5.2-2)

P_x = absolute pressure, measured at wall of plastic venturi at distance x, downstream of the minimum pressure point--for non-cavitating flow

R = bubble radius

$\dot{R}$ = differentiation of R with respect to time

$(Re)_{D_o}$ = Reynolds number, based on test section inlet diameter

R_i = 'initial' bubble radius at the onset of collapse

T_n = ($n = 2, 4, 5, 6, 7, 8$, or 9): measured cavity temperature at a particular station or instrument port in wall of plastic venturi

T_o = bulkstream temperature in degrees Rankine (Kelvin), of liquid entering the test section

V_o = velocity of test liquid at inlet to test section

x = distance measured from minimum pressure point on quarter-round contour along axis of plastic venturi

Greek

α = thermal diffusivity of liquid at inlet to test section

μ = absolute viscosity of liquid at inlet to test section

ρ_o = density of liquid at inlet to test section

Subscripts

C = denotes state of bubble collapse

G = denotes state of bubble growth

ref = reference run (data point), or test conditions, to which a computation is being referenced when attempting to correlate cavitation performance via the similarity equation (5. 3-1)

Superscripts

E1 = exponent on thermal diffusivity ratio in eq (5. 3-1)

E2 = exponent on test section inlet velocity ratio in equation (5. 3-1)

E3 = exponent on cavity length ratio in eq (5. 3-1)

E4 = exponent on test section inlet diameter ratio in eq (5. 3-1)

EN = any one of the exponents used in eq (5. 3-1)

8. REFERENCES

1. Pinkel, I., Hartmann, M. J., Hauser, C. H., Miller, M. J., Ruggeri, R. S., and Soltis, R. F., Pump technology, Chap. VI, pp. 81-101, taken from Conference on Selected Technology for the Petroleum Industry, NASA SP-5053 (1966).
2. Erosion by Cavitation or Impingement, STP-408, 288 pages (1967), available from ASTM, 1916 Race Street, Philadelphia, Pa., 19103.
3. Moore, R. D., and Ruggeri, R. S., Prediction of thermodynamic effects of developed cavitation based on liquid hydrogen and freon-114 data in scaled venturis, NASA Tech. Note D-4899 (Nov. 1968).
4. Ruggeri, R. S., and Moore, R. D., Method for prediction of pump cavitation performance for various liquids, liquid temperatures, and rotative speeds, NASA Tech. Note D-5292 (June 1969).
5. Moore, R. D., Prediction of pump cavitation performance, Proc. Int. Symp. on the Fluid Mechanics and Design of Turbomachinery, Pennsylvania State University, University Park, Pennsylvania, Aug. 30 - Sept. 3, 1970--to be published by NASA.
6. Fisher, R. C., Discussion of "A survey of modern centrifugal pump practice for oilfield and oil refining services" by N. Tetlow, Proc. Inst. Mech. Engrs. 152, 305-306 (Jan. - Dec. 1945).
7. Stahl, H. A., and Stepanoff, A. J., Thermodynamic aspects of cavitation in centrifugal pumps, Trans. ASME 78, No. 8, 1691-1693 (Nov. 1956).

8. Jacobs, R. B., Prediction of symptoms of cavitation, J. Res. Nat. Bur. Stand. (U. S.), 65C (Eng. and Instr.), No. 3, 147-156 (July - Sept. 1961).

9. Hollander, A., Thermodynamic aspects of cavitation in centrifugal pumps, ARS J. 32, 1594-1595 (Oct. 1962).

10. Stepanoff, A. J., Centrifugal and Axial Flow Pumps, pp. 256-265 (John Wiley and Sons, Inc., New York, N. Y., 1957).

11. Stepanoff, A. J., Cavitation properties of liquids, ASME J. of Engr. for Power 86, No. 2, 195-200 (Apr. 1964).

12. Saleman, Victor, Cavitation and NPSH requirements of various liquids, ASME J. of Basic Engr. 81, No. 2, 167-180 (June 1959).

13. Wilcox, W. W., Meng, P. R., and Davis, R. L., Performance of an inducer-impeller combination at or near boiling conditions for liquid hydrogen, Book, Advances in Cryogenic Engineering 8, Ed. K. D. Timmerhaus, pp. 446-455 (Plenum Press, Inc., New York, N. Y. 1963).

14. Spraker, W. A., The effects of fluid properties on cavitation in centrifugal pumps, ASME J. of Engr. for Power 87, No. 3, 309-318 (July 1965).

15. Gelder, T. F., Ruggeri, R. S., and Moore, R. D., Cavitation similarity considerations based on measured pressure and temperature depressions in cavitated regions of freon-114, NASA Tech. Note D-3509 (July 1966).

16. Hord, J., Edmonds, D. K., and Millhiser, D. R., Thermodynamic depressions within cavities and cavitation inception in liquid hydrogen and liquid nitrogen, NASA Rept. CR-72286, (March 1968). Available from NASA, Office of Scientific and Technical Information, AFSS-A, Washington, D. C.

17. Ruggeri, R. S., and Gelder, T. F., Effects of air content and water purity on liquid tension at incipient cavitation in venturi flow, NASA TN D-1459 (1963).

18. Gelder, T. F., Moore, R. D., and Ruggeri, R. S., Incipient cavitation of freon-114 in a tunnel venturi, NASA Tech. Note D-2662 (Feb. 1965).

19. Flow Measurement, Chap. 4, Part 5 - Measurement of quantity of materials, p. 17, PTC, 19.5 (The American Society of Mechanical Engineers, 29 West 39th Street, New York 18, N. Y., Apr. 1959).

20. Hord, J., and Voth, R. O., Tabulated values of cavitation B-factor for helium, H_2, N_2, F_2, O_2, refrigerant 114, and H_2O, Nat. Bur. Stand. (U.S.), Tech. Note 397 (Feb. 1971).

21. Plesset, M. S., Bubble dynamics, California Institute of Tech. Report No. 85-23 (Feb. 1963).

22. Holl, J. W., and Kornhauser, A. L., Thermodynamic effects on desinent cavitation on hemispherical nosed bodies in water at temperatures from 80 F to 260 F, ASME J. of Basic Engr., 44-58 (Mar. 1970).

23. Billet, M. L., Thermodynamic effects on developed cavitation in water and freon-113 (M.S. Thesis, Pennsylvania State Univ., Dept. of Aerospace Engr., University Park, Pa., Mar. 1970).

24. Holl, J. W., and Wislicenus, G. F., Scale effects on cavitation, ASME J. of Basic Engr., 385-398 (Sept. 1961).

25. Rouse, H., and McNown, J.S., Cavitation and pressure distribution on head forms at zero angle of yaw, State Univ. of Iowa, Bulletin 32 (Aug. 1948).

26. Wylie, C. R., Advanced Engineering Mathematics, pp. 175-191 (McGraw-Hill, Inc., New York, N.Y., 1960).

Table A-1a. Experimental developed-cavitation data in venturi using liquid hydrogen (English Units)

Run #	Visual Cavity Length (inches)	T_o (°R)	V_o (ft/sec)	P_o (psia)	P_v (psia)	h_o (ft)	h_v (ft)	K_v	T_2 (°R)	T_4 (°R)	T_5 (°R)	T_6 (°R)	T_7 (°R)	T_8 (°R)	T_9 (°R)
117	3.25	37.21	143.3	35.53	16.52	1162.1	541.7	1.94	32.94	33.16	33.05	33.95	33.84	35.08	36.76
118	2.00	35.80	102.1	20.12	13.12	651.1	424.9	1.40	32.85	33.21	33.46	32.60	34.29	34.72	35.44
119A	2.50	35.77	98.8	19.47	13.04	629.9	422.2	1.37	33.52	33.79	33.93	33.16	34.65	35.26	35.86
119B	3.25	35.77	99.8	19.09	13.04	617.6	422.2	1.26	33.34	33.34	33.43	32.38	33.39	34.18	35.35
120A	1.75	36.79	150.9	35.70	15.46	1163.2	505.1	1.86	33.19	33.80	33.50	33.32	36.04	36.20	36.40
120B	2.75	36.65	149.6	35.15	15.10	1143.8	492.8	1.87	32.47	33.07	32.49	31.70	33.55	34.40	35.71
121A	2.00	41.11	105.6	35.11	29.25	1196.3	997.9	1.15	40.54	40.66	40.66	40.63	40.79	41.00	40.99
121B	3.25	40.99	105.9	33.65	28.76	1145.2	979.6	.95	39.40	40.03	39.91	39.85	40.14	40.50	40.73
122A	1.75	41.22	132.6	39.10	29.68	1333.0	1013.7	1.17	37.80	39.60	39.37	39.24	40.12	41.22	41.04
122B	2.75	41.36	135.9	37.83	30.26	1292.2	1035.1	.90	37.15	38.18	38.07	37.87	39.10	40.57	41.00
123A	1.75	41.04	138.9	39.89	28.97	1356.9	987.4	1.23	37.49	39.24	39.06	38.84	40.14	40.93	40.91
123B	3.25	40.97	139.7	37.49	28.69	1274.7	977.0	.98	36.86	37.55	37.37	37.15	38.63	40.07	40.73
124A	2.25	41.09	101.8	33.89	29.18	1154.8	995.2	.99	40.01	40.43	40.37	40.18	40.48	40.91	41.09
124B	3.25	41.06	104.2	33.49	29.04	1140.8	990.0	.89	38.72	39.56	39.31	39.24	39.55	40.09	40.34
125A	0.75	40.84	106.5	34.97	28.20	1187.9	959.1	1.30	40.48	40.50	40.64	40.55	40.66	40.84	40.82
125B	2.25	40.95	108.5	32.94	28.62	1120.7	974.5	.80	39.37	40.18	40.01	40.00	40.30	40.88	41.04
126A	1.75	37.17	172.6	43.59	16.42	1423.7	538.5	1.91	33.03	33.57	33.66	32.53	35.95	36.38	36.45
126B	3.25	36.92	173.0	42.84	15.77	1396.1	516.0	1.89	32.35	32.78	32.51	30.87	32.89	33.50	35.15
127A	2.63	37.08	174.9	43.81	16.19	1429.6	530.4	1.89	32.71	33.05	32.58	31.64	33.62	34.06	36.07
127B	3.25	37.04	173.0	42.92	16.09	1400.3	527.2	1.88	32.67	33.05	32.36	31.28	32.92	33.71	35.42
128A	2.50	40.32	163.1	43.99	26.24	1483.1	887.5	1.44	35.89	36.36	36.00	35.44	37.44	39.08	39.69
128B	3.50	40.32	168.4	42.69	26.24	1439.6	887.5	1.25	35.84	36.13	35.50	34.85	36.49	37.37	38.83
129A	2.37	40.34	166.7	43.54	26.31	1468.4	889.9	1.34	36.34	36.79	36.34	36.05	38.22	39.96	40.14
129B	3.25	40.21	166.8	43.69	25.85	1471.3	873.2	1.38	35.64	36.00	35.39	34.79	36.20	37.19	38.61
130A	2.00	37.21	190.3	51.14	16.52	1669.1	541.7	2.00	32.99	33.50	33.19	31.97	35.03	36.29	36.49
130B	3.25	37.24	190.7	50.89	16.61	1661.5	545.0	1.98	32.78	33.34	32.85	31.05	32.72	33.34	35.26
131A	2.00	40.73	192.1	55.09	27.79	1862.3	943.9	1.60	36.11	36.54	36.16	35.68	38.70	40.23	40.25
131B	3.25	40.57	192.4	54.74	27.17	1847.2	921.5	1.61	35.77	36.13	35.48	34.22	36.09	37.58	39.29
132A	1.25	40.48	187.6	55.69	26.84	1877.1	909.3	1.77	36.43	37.01	37.15	38.12	40.34	40.66	40.30
132B	3.25	40.45	189.8	54.36	26.70	1832.0	904.4	1.66	35.73	36.20	35.28	34.27	35.95	37.06	38.75
133	3.50	37.15	194.0	52.09	16.37	1699.0	536.9	1.99	32.56	33.16	32.76	31.45	32.76	32.96	34.49
134	2.00	37.24	192.7	52.24	16.61	1705.3	545.0	2.01	32.92	33.50	33.28	31.91	34.61	36.49	36.74

Table A-1a. (Continued)

Run #	P_2 (psia)	P_4 (psia)	P_5 (psia)	P_6 (psia)	P_7 (psia)	P_8 (psia)	P_9 (psia)	$P_{2,T}$ (psia)	$P_{4,T}$ (psia)	$P_{5,T}$ (psia)	$P_{6,T}$ (psia)	$P_{7,T}$ (psia)	$P_{8,T}$ (psia)	$P_{9,T}$ (psia)
117	8.13	8.43	8.73	9.13	10.03	12.03	18.63	7.79	8.12	7.95	9.44	9.25	11.58	15.37
118	8.52	8.89	9.55	10.72	13.12	15.65	17.32	7.65	8.20	8.61	7.28	10.05	10.87	12.33
119A	8.65	9.12	9.60	10.92	13.05	15.37	16.85	8.70	9.15	9.40	8.12	10.73	11.95	13.24
119B	7.92	8.14	8.44	8.94	9.84	11.89	14.34	8.41	8.41	8.55	6.97	8.49	9.85	12.14
120A	8.54	9.10	9.70	11.13	19.35	25.20	29.00	8.18	9.19	8.67	8.38	13.64	14.02	14.49
120B	7.70	8.30	8.45	8.90	9.95	13.55	22.00	7.10	7.98	7.12	6.05	8.76	10.25	12.92
121A	25.31	27.26	27.24	28.44	30.19	31.49	33.08	27.04	27.51	27.51	27.38	27.99	28.83	28.76
121B	21.65	24.85	24.85	26.07	27.85	29.46	31.17	23.03	25.20	24.76	24.57	25.59	26.91	27.79
122A	18.80	24.80	24.55	26.55	29.80	32.40	35.25	18.13	23.70	22.92	22.50	25.52	29.68	28.97
122B	16.63	18.43	20.38	21.53	24.73	28.73	32.08	16.37	19.21	18.90	18.33	22.03	27.17	28.83
123A	17.49	23.89	23.42	25.59	29.47	32.19	35.42	17.28	22.50	21.92	21.23	25.59	28.55	28.48
123B	15.39	16.89	17.69	19.24	21.99	25.84	30.14	15.64	17.43	16.94	16.37	20.56	25.33	27.79
124A	22.84	25.39	25.34	26.59	28.39	29.79	31.69	25.14	26.64	26.44	25.72	26.84	28.48	29.18
124B	21.04	24.49	24.39	25.74	27.54	29.19	30.89	20.84	23.58	22.74	22.50	23.52	25.40	26.31
125A	26.18	27.27	27.35	28.49	30.12	31.37	33.02	26.84	26.91	27.45	27.11	27.51	28.20	28.13
125B	20.37	24.04	23.84	24.99	26.79	28.57	30.29	22.92	25.72	25.14	25.08	26.18	28.34	28.97
126A	8.99	9.49	9.64	11.09	18.64	29.84	34.64	7.92	8.79	8.94	7.17	13.44	14.44	14.62
126B	7.94	8.54	8.59	8.59	9.24	11.29	18.09	6.92	7.54	7.15	5.07	7.70	8.67	11.73
127A	8.41	8.86	9.26	9.51	11.06	17.18	29.21	7.43	7.95	7.25	5.99	8.88	9.63	13.73
127B	7.76	8.25	8.62	8.42	9.02	11.45	17.42	7.38	7.95	6.94	5.55	7.76	9.03	12.29
128A	13.44	14.59	15.04	16.14	19.09	26.49	33.54	13.32	14.40	13.56	12.33	17.14	21.97	24.01
128B	12.39	13.59	13.39	13.99	15.59	18.89	24.69	13.20	13.85	12.45	11.11	14.70	16.94	21.17
129A	12.94	14.24	14.89	16.34	20.74	29.74	34.74	14.36	15.46	14.36	13.68	19.40	24.95	25.59
129B	12.49	13.59	14.19	14.59	16.39	20.39	26.39	12.76	13.56	12.22	11.01	13.90	16.47	20.50
130A	8.64	9.24	9.84	10.44	14.79	32.44	38.39	7.87	8.67	8.18	6.40	11.47	14.23	14.70
130B	7.34	8.44	8.89	8.39	8.74	10.59	16.99	7.54	8.41	7.65	5.27	7.46	8.41	11.95
131A	12.99	14.09	15.14	16.74	23.14	36.84	43.29	13.81	14.83	13.93	12.84	20.78	25.91	25.98
131B	12.04	13.34	13.54	13.19	14.74	19.69	29.59	13.04	13.85	12.41	9.92	13.77	17.53	22.68
132A	13.74	15.94	18.34	26.14	36.54	41.34	46.79	14.57	16.00	16.37	19.05	26.31	27.51	26.18
132B	12.46	13.86	13.81	13.24	14.86	18.86	26.91	12.96	14.02	11.99	10.02	13.44	16.14	20.95
133	8.44	9.44	9.59	8.89	8.89	10.29	14.34	7.22	8.12	7.51	5.74	7.51	7.81	10.42
134	8.74	9.34	9.64	9.54	11.84	23.69	36.79	7.76	8.67	8.32	6.33	10.66	14.70	15.32

Table A-1a. (Continued)

Run #	h_2 (ft)	h_4 (ft)	h_5 (ft)	h_6 (ft)	h_7 (ft)	h_8 (ft)	h_9 (ft)	$h_{2,T}$ (ft)	$h_{4,T}$ (ft)	$h_{5,T}$ (ft)	$h_{6,T}$ (ft)	$h_{7,T}$ (ft)	$h_{8,T}$ (ft)	$h_{9,T}$ (ft)
117	257.7	267.6	277.6	290.8	320.8	388.1	615.5	246.4	257.4	251.8	301.0	294.7	372.9	502.0
118	270.6	282.9	304.8	343.9	425.0	511.8	569.7	241.9	260.2	273.6	229.7	321.5	348.8	398.3
119A	274.9	290.5	306.5	350.6	422.7	502.1	553.4	276.6	291.7	300.0	257.4	344.1	385.4	429.0
119B	250.8	258.1	268.0	284.5	314.5	383.3	466.7	266.9	266.9	271.7	219.6	269.7	314.9	391.8
120A	271.3	289.8	309.8	357.7	640.8	849.7	988.5	259.3	292.7	275.6	265.9	442.9	455.7	471.7
120B	243.6	263.4	268.3	283.2	318.1	439.7	734.7	223.8	252.8	224.6	189.8	278.6	328.1	418.1
121A	853.7	924.7	923.9	967.9	1032.5	1080.8	1140.2	916.6	933.9	933.9	929.0	951.5	982.2	979.6
121B	722.2	837.1	837.1	881.3	946.3	1005.5	1068.8	771.7	849.8	833.7	826.9	863.8	911.7	943.9
122A	621.5	835.2	826.2	898.8	1018.0	1114.7	1222.0	597.9	795.6	767.4	752.6	861.5	1013.7	987.4
122B	545.7	608.5	677.2	718.0	832.7	978.6	1102.8	536.9	635.9	624.8	605.0	735.8	921.5	982.2
123A	575.6	802.4	785.5	863.9	1006.8	1106.9	1228.4	568.4	752.6	731.7	707.3	863.8	971.9	969.3
123B	502.8	554.8	582.6	636.9	734.4	872.9	1030.6	511.3	573.6	556.6	536.9	683.5	854.5	943.9
124A	764.7	856.6	854.8	900.2	966.1	1017.7	1088.2	847.5	902.0	894.7	868.5	909.3	969.3	995.2
124B	700.6	824.1	820.4	869.3	934.9	995.5	1058.4	693.3	791.2	761.0	752.6	789.1	856.8	889.9
125A	885.3	925.0	928.0	969.7	1029.9	1076.3	1137.9	909.3	911.7	931.4	919.1	933.9	959.1	956.6
125B	676.8	807.8	800.6	842.1	907.5	972.7	1036.2	767.4	868.5	847.5	845.2	885.1	964.2	987.4
126A	286.2	302.8	307.8	356.3	615.9	1019.5	1198.9	250.9	279.5	284.5	226.3	435.9	470.3	476.2
126B	251.5	271.3	272.9	272.9	294.5	363.1	596.6	217.9	238.4	225.4	158.0	243.7	275.6	377.9
127A	267.0	281.9	295.2	303.5	355.3	564.8	996.3	234.9	251.8	228.8	187.6	282.5	307.4	445.7
127B	245.6	261.7	273.9	267.3	287.2	368.5	573.2	233.1	251.8	218.8	173.4	245.5	287.6	397.0
128A	435.9	475.3	490.8	528.7	631.7	896.6	1157.5	431.7	468.8	440.1	398.3	563.4	733.8	806.7
128B	400.2	441.1	434.2	454.7	509.7	624.6	831.3	427.6	450.0	402.2	357.1	479.2	556.6	705.3
129A	418.9	463.3	485.6	535.7	689.9	1015.8	1202.7	467.3	505.1	467.3	444.3	650.0	840.6	863.8
129B	403.6	441.1	461.6	475.3	537.4	677.5	892.9	412.7	440.1	394.4	353.5	416.0	540.1	681.5
130A	274.6	294.5	314.5	334.5	482.2	1116.2	1341.7	249.1	275.6	259.3	201.2	369.2	462.9	479.2
130B	231.8	268.0	282.9	266.3	277.9	339.6	558.2	238.4	266.9	241.9	164.6	235.7	266.9	385.4
131A	420.6	458.2	494.2	549.5	775.5	1284.4	1531.8	448.6	483.7	452.8	415.4	691.3	875.6	878.0
131B	388.4	432.5	439.4	427.4	480.5	652.8	1010.3	422.2	450.0	400.9	317.1	447.1	577.0	758.9
132A	446.2	521.8	605.4	883.8	1271.0	1455.7	1670.0	474.7	524.0	536.9	630.3	889.9	933.9	885.1
132B	402.6	450.3	448.6	429.1	484.6	623.6	911.9	419.4	455.7	386.7	320.4	435.9	528.8	697.3
133	268.0	301.1	306.1	282.9	282.9	329.5	466.7	228.0	257.4	237.5	179.7	237.5	247.3	333.8
134	277.9	297.8	307.8	304.5	381.6	795.2	1280.5	245.5	275.6	264.0	198.9	341.8	479.2	500.4

Table A-1b. Experimental developed - cavitation data in venturi using liquid hydrogen (SI Units)

Run #	Visual Cavity Length (cm)	T_o (°K)	V_o (m/sec)	P_o (N/cm^2)	P_v (N/cm^2)	h_o (m)	h_v (m)	K_v	T_2 (°K)	T_4 (°K)	T_5 (°K)	T_6 (°K)	T_7 (°K)	T_8 (°K)	T_9 (°K)
117	8.26	20.67	43.7	24.50	11.39	354.2	165.1	1.94	18.30	18.42	18.36	18.86	18.80	19.49	20.42
118	5.08	19.89	31.1	13.87	9.04	198.4	129.5	1.40	18.25	18.45	18.59	18.11	19.05	19.29	19.69
119A	6.35	19.87	30.1	13.42	8.99	192.0	128.7	1.37	18.62	18.77	18.85	18.42	19.25	19.59	19.92
119B	8.26	19.87	30.4	13.16	8.99	188.3	128.7	1.26	18.52	18.52	18.57	17.99	18.55	18.99	19.64
120A	4.45	20.44	46.0	24.61	10.66	354.5	153.9	1.86	18.44	18.78	18.61	18.51	20.02	20.11	20.22
120B	6.99	20.36	45.6	24.24	10.41	348.6	150.2	1.87	18.04	18.37	18.05	17.61	18.64	19.11	19.84
121A	5.08	22.84	32.2	24.21	20.17	364.6	304.1	1.15	22.52	22.59	22.59	22.57	22.66	22.78	22.77
121B	8.26	22.77	32.3	23.20	19.83	349.1	298.6	.95	21.89	22.24	22.17	22.14	22.30	22.50	22.63
122A	4.45	22.90	40.4	26.96	20.47	406.3	309.0	1.17	21.00	22.00	21.87	21.80	22.29	22.90	22.80
122B	6.99	22.98	41.4	26.08	20.86	393.9	315.5	.90	20.64	21.21	21.15	21.04	21.72	22.54	22.78
123A	4.45	22.80	42.3	27.50	19.97	413.6	301.0	1.23	20.83	21.80	21.70	21.58	22.30	22.74	22.73
123B	8.26	22.76	42.6	25.85	19.78	388.5	297.8	.98	20.48	20.86	20.76	20.64	21.46	22.26	22.63
124A	5.72	22.83	31.0	23.37	20.12	352.0	303.3	.99	22.23	22.46	22.43	22.32	22.49	22.73	22.83
124B	8.26	22.81	31.8	23.09	20.02	347.7	301.8	.89	21.51	21.98	21.84	21.80	21.97	22.27	22.41
125A	1.91	22.69	32.5	24.11	19.44	362.1	292.3	1.30	22.49	22.50	22.58	22.53	22.59	22.69	22.68
125B	5.72	22.75	33.1	22.71	19.73	341.6	297.0	.80	21.87	22.32	22.23	22.22	22.39	22.71	22.80
126A	4.45	20.65	52.6	30.05	11.32	433.9	164.1	1.91	18.35	18.65	18.70	18.07	19.97	20.21	20.25
126B	8.26	20.51	52.7	29.54	10.87	425.5	157.3	1.89	17.97	18.21	18.06	17.15	18.27	18.61	19.53
127A	6.68	20.60	53.3	30.21	11.16	435.7	161.7	1.89	18.17	18.36	18.10	17.58	18.68	18.92	20.04
127B	8.26	20.58	52.7	29.59	11.10	426.8	160.7	1.88	18.15	18.36	17.98	17.38	18.29	18.73	19.68
128A	6.35	22.40	49.7	30.33	18.09	452.1	270.5	1.44	19.94	20.20	20.00	19.69	20.80	21.71	22.05
128B	8.89	22.40	51.3	29.43	18.09	438.8	270.5	1.25	19.91	20.07	19.72	19.36	20.27	20.76	21.57
129A	6.02	22.41	50.8	30.02	18.14	447.6	271.2	1.34	20.19	20.44	20.19	20.03	21.23	22.20	22.30
129B	8.26	22.34	50.8	30.12	17.82	448.5	266.2	1.38	19.80	20.00	19.66	19.33	20.09	20.66	21.45
130A	5.08	20.67	58.0	35.26	11.39	508.7	165.1	2.00	18.33	18.61	18.44	17.76	19.46	20.16	20.27
130B	8.26	20.69	58.1	35.09	11.45	506.4	166.1	1.98	18.21	18.52	18.25	17.25	18.18	18.52	19.59
131A	5.08	22.63	58.5	37.98	19.16	567.6	287.7	1.60	20.06	20.30	20.09	19.82	21.50	22.35	22.36
131B	8.26	22.54	58.6	37.74	18.74	563.0	280.9	1.61	19.87	20.07	19.71	19.01	20.05	20.88	21.83
132A	3.18	22.49	57.2	38.40	18.50	572.2	277.1	1.77	20.24	20.56	20.64	21.18	22.41	22.59	22.39
132B	8.26	22.47	57.8	37.48	18.41	558.4	275.7	1.66	19.85	20.11	19.60	19.04	19.97	20.59	21.53
133	8.89	20.64	59.1	35.91	11.29	517.9	163.6	1.99	18.09	18.42	18.20	17.47	18.20	18.31	19.16
134	5.08	20.69	58.7	36.02	11.45	519.8	166.1	2.01	18.29	18.61	18.49	17.73	19.23	20.27	20.41

Table A-1b. (Continued)

Run #	P_2 (N/cm^2)	P_4 (N/cm^2)	P_5 (N/cm^2)	P_6 (N/cm^2)	P_7 (N/cm^2)	P_8 (N/cm^2)	P_9 (N/cm^2)	$P_{2,T}$ (N/cm^2)	$P_{4,T}$ (N/cm^2)	$P_{5,T}$ (N/cm^2)	$P_{6,T}$ (N/cm^2)	$P_{7,T}$ (N/cm^2)	$P_{8,T}$ (N/cm^2)	$P_{9,T}$ (N/cm^2)
117	5.61	5.81	6.02	6.29	6.92	8.29	12.84	5.37	5.60	5.48	6.51	6.38	7.99	10.59
118	5.87	6.13	6.58	7.39	9.05	10.79	11.94	5.27	5.66	5.94	5.02	6.93	7.49	8.50
119A	5.96	6.29	6.62	7.53	9.00	10.60	11.62	6.00	6.31	6.48	5.60	7.40	8.24	9.13
119B	5.46	5.61	5.82	6.16	6.78	8.20	9.89	5.80	5.80	5.90	4.80	5.86	6.79	8.37
120A	5.89	6.27	6.69	7.67	13.34	17.37	19.99	5.64	6.33	5.98	5.78	9.41	9.67	9.99
120B	5.31	5.72	5.83	6.14	6.86	9.34	15.17	4.89	5.50	4.91	4.17	6.04	7.07	8.91
121A	17.45	18.80	18.78	19.61	20.82	21.71	22.81	18.64	18.97	18.97	18.88	19.30	19.88	19.83
121B	14.93	17.13	17.13	17.97	19.20	20.31	21.49	15.88	17.38	17.07	16.94	17.64	18.55	19.16
122A	12.96	17.10	16.93	18.31	20.55	22.34	24.30	12.50	16.34	15.80	15.51	17.60	20.47	19.97
122B	11.47	12.71	14.05	14.84	17.05	19.81	22.12	11.29	13.24	13.03	12.64	15.19	18.74	19.88
123A	12.06	16.47	16.15	17.64	20.32	22.19	24.42	11.92	15.51	15.11	14.64	17.64	19.68	19.64
123B	10.61	11.65	12.20	13.27	15.16	17.82	20.78	10.78	12.02	11.68	11.29	14.17	17.47	19.16
124A	15.75	17.51	17.47	18.33	19.57	20.54	21.85	17.33	18.37	18.23	17.73	18.50	19.64	20.12
124B	14.51	16.89	16.82	17.75	18.99	20.13	21.30	14.37	16.26	15.68	15.51	16.22	17.51	18.14
125A	18.05	18.80	18.86	19.64	20.77	21.63	22.77	18.50	18.55	18.92	18.69	18.97	19.44	19.40
125B	14.04	16.57	16.44	17.23	18.47	19.70	20.88	15.80	17.73	17.33	17.29	18.05	19.54	19.97
126A	6.20	6.54	6.65	7.65	12.85	20.57	23.88	5.46	6.06	6.16	4.95	9.27	9.96	10.08
126B	5.47	5.89	5.92	5.92	6.37	7.78	12.47	4.77	5.20	4.93	3.50	5.31	5.98	8.09
127A	5.80	6.11	6.38	6.56	7.63	11.85	20.14	5.13	5.48	5.00	4.13	6.12	6.64	9.46
127B	5.35	5.69	5.94	5.81	6.22	7.89	12.01	5.09	5.48	4.79	3.82	5.35	6.23	8.48
128A	9.27	10.06	10.37	11.13	13.16	18.26	23.13	9.18	9.93	9.35	8.50	11.82	15.15	16.55
128B	8.54	9.37	9.23	9.65	10.75	13.02	17.02	9.10	9.55	8.58	7.66	10.14	11.68	14.60
129A	8.92	9.82	10.27	11.27	14.30	20.51	23.95	9.90	10.66	9.90	9.44	13.32	17.20	17.64
129B	8.61	9.37	9.78	10.06	11.30	14.06	18.20	8.80	9.35	8.42	7.59	9.57	11.35	14.14
130A	5.96	6.37	6.78	7.20	10.20	22.37	26.47	5.42	5.98	5.64	4.42	7.91	9.81	10.14
130B	5.06	5.82	6.13	5.78	6.03	7.30	11.71	5.20	5.80	5.27	3.64	5.14	5.80	8.24
131A	8.96	9.71	10.44	11.54	15.95	25.40	29.85	9.52	10.23	9.61	8.85	14.33	17.87	17.91
131B	8.30	9.20	9.34	9.09	10.16	13.58	20.40	8.99	9.55	8.56	6.84	9.49	12.09	15.64
132A	9.47	10.99	12.64	18.02	25.19	28.50	32.26	10.05	11.03	11.29	13.14	18.14	18.97	18.05
132B	8.59	9.56	9.52	9.13	10.25	13.00	18.55	8.93	9.67	8.27	6.91	9.27	11.13	14.44
133	5.82	6.51	6.61	6.13	6.13	7.09	9.89	4.98	5.60	5.18	3.96	5.18	5.39	7.18
134	6.03	6.44	6.65	6.58	8.16	16.33	25.37	5.35	5.98	5.74	4.37	7.35	10.14	10.56

Table A-1b. (Continued)

Run #	h_2 (m)	h_4 (m)	h_5 (m)	h_6 (m)	h_7 (m)	h_8 (m)	h_9 (m)	$h_{2,T}$ (m)	$h_{4,T}$ (m)	$h_{5,T}$ (m)	$h_{6,T}$ (m)	$h_{7,T}$ (m)	$h_{8,T}$ (m)	$h_{9,T}$ (m)
117	78.6	81.6	84.6	88.6	97.8	118.3	187.6	75.1	78.5	76.8	91.7	89.8	113.7	153.0
118	82.5	86.2	92.9	104.8	129.6	156.0	173.7	73.7	79.3	83.4	70.0	98.0	106.3	121.4
119A	83.8	88.5	93.4	106.9	128.8	153.1	168.7	84.3	88.9	91.4	78.5	104.9	117.5	130.8
119B	76.5	78.7	81.7	86.7	95.9	116.8	142.3	81.3	81.3	82.8	66.9	82.2	96.0	119.4
120A	82.7	88.3	94.4	109.0	195.3	259.0	301.3	79.0	89.2	84.0	81.0	135.0	138.9	143.8
120B	74.2	80.3	81.8	86.3	97.0	134.0	223.9	68.2	77.0	68.5	57.9	84.9	100.0	127.4
121A	260.2	281.8	281.6	295.0	314.7	329.4	347.5	279.4	284.7	284.7	283.1	290.0	299.4	298.6
121B	220.1	255.1	255.1	268.6	288.4	306.5	325.8	235.2	259.0	254.1	252.0	263.3	277.9	287.7
122A	189.4	254.6	251.8	273.9	310.3	339.8	372.5	182.2	242.5	233.9	229.4	262.6	309.0	301.0
122B	166.3	185.5	206.4	218.8	253.8	298.3	336.1	163.6	193.8	190.4	184.4	224.3	280.9	299.4
123A	175.5	244.6	239.4	263.3	306.6	337.4	374.4	173.3	229.4	223.0	215.6	263.3	296.2	295.4
123B	153.3	169.1	177.6	194.1	223.8	266.1	314.1	155.8	174.8	169.7	163.6	208.3	260.4	287.7
124A	233.1	261.1	260.5	274.4	294.5	310.2	331.7	258.3	274.9	272.7	264.7	277.1	295.4	303.3
124B	213.5	251.2	250.1	265.0	285.0	303.4	322.6	211.3	241.2	232.0	229.4	240.5	261.2	271.2
125A	269.8	281.9	282.8	295.6	313.9	328.1	346.8	277.1	277.9	283.9	280.1	284.7	292.3	291.6
125B	206.3	246.2	244.0	256.7	276.6	296.5	315.8	233.9	264.7	258.3	257.6	269.8	293.9	301.0
126A	87.2	92.3	93.8	108.6	187.7	310.7	365.4	76.5	85.2	86.7	69.0	132.9	143.3	145.1
126B	76.7	82.7	83.2	83.2	89.8	110.7	181.8	66.4	72.7	68.7	48.2	74.3	84.0	115.2
127A	81.4	85.9	90.0	92.5	108.3	172.2	303.7	71.6	76.8	69.7	57.2	86.1	93.7	135.9
127B	74.8	79.8	83.5	81.5	87.5	112.3	174.7	71.1	76.8	66.7	52.8	74.8	87.7	121.0
128A	132.9	144.9	149.6	161.2	192.5	273.3	352.8	131.6	142.9	134.1	121.4	171.7	223.7	245.9
128B	122.0	134.4	132.4	138.6	155.4	190.4	253.4	130.3	137.2	122.6	108.8	146.1	169.7	215.0
129A	127.7	141.2	148.0	163.3	210.3	309.6	366.6	142.4	153.9	142.4	135.4	198.5	256.2	263.3
129B	123.0	134.4	140.7	144.9	163.8	206.5	272.2	125.8	134.1	120.2	107.8	126.8	164.6	207.7
130A	83.7	89.8	95.9	102.0	147.0	340.2	409.0	75.9	84.0	79.0	61.3	112.5	141.1	146.1
130B	70.6	81.7	86.2	81.2	84.7	103.5	170.2	72.7	81.3	73.7	50.2	71.9	81.3	117.5
131A	128.2	139.6	150.6	167.5	236.4	390.9	466.9	136.7	147.4	138.0	126.6	210.7	266.9	267.6
131B	118.4	131.8	133.9	130.3	146.4	199.0	307.9	128.7	137.2	122.2	96.6	136.3	175.9	231.3
132A	136.0	159.1	184.5	269.4	387.4	443.7	509.0	144.7	159.7	163.6	192.1	271.2	284.7	269.8
132B	122.7	137.2	136.7	130.8	147.7	190.1	277.9	127.8	138.9	117.9	97.6	132.9	161.2	212.5
133	81.7	91.8	93.3	86.2	86.2	100.4	142.3	69.5	78.5	72.4	54.8	72.4	75.4	101.7
134	84.7	90.8	93.8	92.8	116.3	242.4	390.3	74.8	84.0	80.5	60.6	104.2	146.1	152.5

Appendix B: Thermocouple fabrication procedure

I. Support tubes

A. Use 1/16-inch dia. x 0.012-inch wall stainless steel tubing.

B. Cut 1.25-inch lengths of this tubing with jewelers file.

C. Hold a tubing length in pin vise and deburr tubing with $\approx$ 1/16-inch diameter drill held in another pin vise.

D. Soak these support tubes in trichloroethylene to clean.

II. Thermocouple junctions

A. Skin thermocouple wire insulation with #320 abrasive cloth.

B. Tin the Chromel[5] wire using stainless steel soldering flux and solid core (50/50) solder. Wash off flux.

C. Twist Chromel-Au (0.07 at. percent Fe) wires together to form junction and solder using resin-core radio solder. Use voltage-controlled soldering iron and do not get Au wire too hot--use just enough heat to melt solder.

D. Clean soldered junctions with a solvent, and then coat all uninsulated surfaces with G. E. Varnish.[5]

III. Support tube and thermocouple junction assembly

A. Wipe wires with solvent (avoid varnish).

B. Thread junctions and suitable length of extension wire into 1/16-inch diameter support tubes.

C. Attach a transparent vacuum hose to the junction (sensor) end of the assembly.

D. Mix epoxy: Emerson and Cuming, Inc., Stycast 2850 GT[5] with room temperature cure activator.

---

[5] Identification of a manufacturer and a manufacturer's product has been necessary to make the results of this work meaningful and in no way implies a recommendation or endorsement by the National Bureau of Standards, or by the National Aeronautics and Space Administration.

E. Apply epoxy to the non-junction end of the support tube; then use the vacuum-assist and manipulate the thermocouple wires in the tube until epoxy appears at the junction end (inside transparent vacuum hose) of the support tube.

F. Remove vacuum hose and excess epoxy from both ends of the support tube.

G. Make final placement of junctions and allow adequate cure time. Junctions should project slightly from the support tubes and should be visibly centered in the support tube; i. e. , the thermocouple wire should not be in contact with the support tube on either end.

IV. Installation

A. The 1/16-inch diameter thermocouple probes are then inserted into the plastic venturi through compression fittings as indicated in figure 3. 6.

The reference thermocouples (figure 3. 7) were fabricated in the same fashion, except that all of the 1/16-inch diameter support tubes were first soldered, with parallel axes, inside of a single 1/4-inch diameter support tube. This precaution assures that all of the reference thermocouple junctions will be at the same temperature.

Appendix C: Computer programs for correlation of developed cavity data

This appendix outlines the details of the two digital computer programs used to determine the exponents on eq (5. 3-1). The programs will be described, in turn, and will be referred to as (1) the variation-of-parameter solution and (2) the Bjorck solution. The Bjorck solution is a sophisticated "least-squares" method, and the variation-of-parameter solution is a basic least-squares approach. The latter program uses the method of "steepest descent" to locate a minima in the selected ordinate--in this case, standard deviation in B-factor. The Bjorck program always finds the absolute minimum ordinate, while the variation-of-parameter program may find a local minima; however, the method of steepest descent tends to locate the absolute minimum. The Bjorck program consumes little machine-time and simultaneously determines, without bound, all of the exponents in eq (5. 3-1). The parametric program is much slower and incrementally varies one exponent at a time, conveniently providing realistic bounds on the exponents. Providing bounds for the exponents is a necessary feature when correlating data with only a slight variation in one or more of the physical parameters, e. g. , α, V_o, or ℓ.

To illustrate this point, consider a group of data where α varies by only 5 percent and the data scatter is about 5 percent--the Bjorck program may pick E1 = 1. 0 or -1. 0, but by selecting the incremental range and initial value of E1, we can force the variation-of-parameter program to pick a value for E1 between any limits that we choose, e. g. , between 0. 2 and -0. 2. Because the variation-of-parameter solution may not find the absolute minimum ordinate, the Bjorck program provides a ready check on the parametric solution.

For data with appreciable variation of all physical parameters, the Bjorck program is far superior, because it is much faster and more reliable; therefore, this program is ideal for most fluid-to-fluid correlations. The variation-of-parameter solution is usually best for single fluid correlations where the physical parameter data may not vary much.

To feel confident that the best solution has been obtained, one must possess a basic understanding of the problem and exercise considerable intuition, i.e., curve-fitting is still an art! While the digital computer is a powerful tool that can rapidly solve complex and cumbersome problems, it is restrained by the mathematical techniques at our disposal. The method of 'least-squares' is no exception, and one should be aware of certain pitfalls; some of the hazards of attempting to blindly fit data with this technique will be revealed herein. There are two practical reasons why the least squares method [26] is used extensively for data-fitting problems: (1) the condition of minimizing the sum of the squares of the deviations is a convenient and efficient method of handling large quantities of data with computer routines, and (2) statistical theory claims that when certain necessary least squares conditions are met, the least squares solution is the 'best' obtainable.

Variation-of-parameter solution: This program uses the least squares technique and the method of steepest descent to locate a minima. To fully understand how the computer program is formulated, we rewrite eq (5.3-1) in abbreviated form,

$$B = B_{ref} \left(\alpha_{ref} / \alpha \right)^{E1} \left(V_o / V_{o,ref} \right)^{E2} \ldots, \text{ etc.} \qquad \text{(C-1)}$$

Note that in the computer program, see page C11, B = BCONV, $B_{ref} = B_t$ = BFLASH, for the selected reference run, α_{ref} = ALPHA (REF), etc. In the discussion that follows, computer-program symbols will always appear in capital letters and the symbol, *, will denote multiplication. The method of least squares is applicable to non-linear problems if they can be converted into equations where the parameters enter linearly. Equation (C-1) can then be handled by this technique if it is linearized and if we can reasonably estimate an approximate solution, E1 = E1,0, E2 = E2,0, etc. Wylie [26] shows that the deviation in B is given by a Taylor's series expansion about the approximate solution point,

$$\delta B = \frac{\partial f}{\partial E1}\Bigg|_{E1,0} * \delta E1 + \frac{\partial f}{\partial E2}\Bigg|_{E2,0} * \delta E2 + \ldots, \text{ etc.}, \qquad (C\text{-}2)$$

where B = f(E1, E2, E3, ..., etc.) and δE1 to δEN is the exponent increment used in the computer program. Recall that B_{ref}, α, V_o, etc., are input data and the exponents, E1 to EN are to be determined.

Performing the indicated differentiation on the first two terms of (C-1), we obtain

$$\delta B = \left\{ B_{ref} \left(\frac{\alpha_{ref}}{\alpha}\right)^{E1} \left(\frac{V_o}{V_{o,ref}}\right)^{E2} \ell n\left(\frac{\alpha_{ref}}{\alpha}\right) \right\} \delta E1 + \left\{ B_{ref} \left(\frac{\alpha_{ref}}{\alpha}\right)^{E1} \left(\frac{V_o}{V_{o,ref}}\right)^{E2} \ell n\left(\frac{V_o}{V_{o,ref}}\right) \right\} \delta E2 .$$

This expression then reduces to

$$\delta B = BCONV \left\{ \ell n\left(\frac{\alpha_{ref}}{\alpha}\right) * \delta E1 + \ell n\left(\frac{V_o}{V_{o,ref}}\right) * \delta E2 \right\}, \qquad (C\text{-}3)$$

for the two terms considered. Now if we only permit one exponent to vary at a time, e.g., E1, we may write

$$\delta B = BCONV * \ell n\left(\frac{\alpha_{ref}}{\alpha}\right) * \delta E1 \ . \qquad (C\text{-}4)$$

Similar expressions may be written for each exponent (EN) and its accompanying log term. Using (C-4), we obtain an equation of condition for each data point, and every equation in this system is linear in δEN; the $\frac{\partial f}{\partial EN}\Big|_{EN,0}$ becomes the coefficients in this linear system of equations. The method of least squares is then applied directly to this system--each equation of condition is multiplied by the coefficient of the variable in that equation and summed [26]--to obtain

$$\sum \frac{\partial f}{\partial EN} * \delta B = \sum \left\{ \left(\frac{\partial f}{\partial EN}\right)^2 * \delta EN \right\} \ . \qquad (C\text{-}5)$$

This expression derives directly from application of the least squares method to eq (C-2), recalling that only one exponent is being varied. Upon completion of this computation, the estimated solution is corrected by an appropriate incremental value and the entire process cycled until the calculated and estimated exponent values converge. In this approach, we are minimizing on the expression in (C-5), a necessary condition for minimization of the variance in B. We may, in fact, combine (C-2) and (C-5) under the constraint of single exponent variation, to obtain

$$\sum (\delta B)^2 = \sum \left\{ \left(\frac{\partial f}{\partial EN}\right)^2 \left(\delta EN\right)^2 \right\} \ . \qquad (C\text{-}6)$$

Equation (C-6) will be recognized as the familiar "propagation of variance" rule, and (C-6) is minimized in the conventional least squares solution; i.e., variance in B is minimized. The term BCONV * ℓn (Ratio) in (C-3) and (C-4) may then be viewed as an 'apparent weight factor', applicable to this particular problem where each exponent is

altered sequentially. For a numerical solution, we will increment one of the exponents at a time, until all of the exponents have been changed--this process will be repeated several times to provide sufficient range for each exponent--then this incrementing process is repeated in ever-decreasing incremental steps. Repeating this process a sufficient number of times with appropriate sized increments results in the "best" solution possible. This program uses two criteria to evaluate the quality of the data-fit, (1) MNBDIFPC = the mean percent difference in B and (2) STDDEV = the standard deviation in B. These two terms are defined as follows:

$$\text{MNBDIFPC} \equiv \left[\frac{\sum \left\{ \frac{|\text{BDIF}| * 100}{\text{BFLASH}} \right\}}{(\text{NPTS}-1)} \right] ,$$

$$\text{STDDEV} \equiv \left\{ \frac{\sum (\text{BDIF})^2}{(\text{NPTS}-1)} \right\}^{1/2} ,$$

where δ B = BDIF = BCONV-BFLASH and NPTS = number of data points.

This variation-of-parameter program functions as follows:

(1) All input data, including BFLASH, are read and stored in computer memory--statement 1.

(2) The reference run is indicated, and initial estimates for each exponent are read and stored--whether the exponent is to be fixed or varied is determined--statement 3.

(3) The physical parameter ratios are computed and stored--statement 9.

(4) These ratios are then exponentiated--statement 23.

(5) Each exponent is then sequentially incremented in ever-decreasing steps--statement 11 + 1.

(6) STDDEV and MNBDIFPC are evaluated--statements 20 + 2 and 27 + 2, respectively.

(7) Pertinent dimensionless numbers may be computed upon demand--statement 30.

(8) The average value of $K_{c,min}$ is computed--statement 35 + 1.

Pertinent information is printed out as it is generated during the program operation. An option is included that permits calculation of the arithmetic mean "reference data"--statement 51. This calculated "reference run" always provides good results and thus permits a comparative evaluation with actual runs when they are used as the reference data!

Bjorck solution: This program, though sophisticated, is programmed to provide a conventional least-squares solution to data-fitting problems. Because this program simultaneously determines the exponents in (C-1), we must rewrite (C-1) in the conventional 'linear' form; taking the logarithm of both sides of (C-1) yields

$$f(B) = \ell n \left(\frac{B}{B_{ref}} \right) = E1 * \ell n \left(\frac{\alpha_{ref}}{\alpha} \right) + E2 * \ell n \left(\frac{V_o}{V_{o,ref}} \right) + \ldots \text{ etc.} \qquad \text{(C-7)}$$

Recall that the 'propagation of variance' rule requires that

$$\sum (\delta f)^2 = \sum \left(\frac{\partial f}{\partial B} * \delta B \right)^2 . \qquad \text{(C-8)}$$

Now that our original problem is written in 'linear' form (with logarithmic coefficients), minimization of (C-8) results in the 'best' solution of (C-7) in its logarithmic or nonlinear sense. This solution requires that $\sum \left(\frac{\partial f}{\partial B} * \delta B \right)^2$ be minimized, and thus $\sum \left(\frac{BDIF}{BFLASH} \right)^2$ is minimal. The latter term, though different, contains the essential ingredients of MNBDIFPC. To obtain the 'best' solution in the linear sense, i.e., for minimum $\sum (\delta B)^2$, we must multiply the left side of

(C-8) by $1 \Big/ \left(\frac{\partial f}{\partial B}\right)^2$, leaving $\sum(\delta B)^2$ on the right side of (C-8). The $\sum(\delta B)^2$ is then minimized in the Bjorck program, STDDEV is minimal, and the result is the 'best' available in the linear sense of the problem. Differentiating (C-7), we obtain $\left(\frac{\partial f}{\partial B}\right)^2 = 1/B^2$. This term is commonly called the weight function and ideally should be evaluated with BCONV; however, BCONV has not yet been computed, so we must use the isentropic flashing value, BFLASH, for the first computation. Thereafter, the weight factor could be improved by using BCONV; this nicety did not appear to be warranted and is not incorporated in the Bjorck program. Theoretically, the solution to our problem that produces the minimum STDDEV is what we seek, and so the 'weight' function, $(BFLASH)^2$, should be used with all data. When this weight term is neglected, the Bjorck program will return results based on minimum $\sum\left(\frac{BDIF}{BFLASH}\right)^2$; usually, these results do not differ much from those obtained for minimal STDDEV. The Bjorck program functions as follows:

(1) All input data, including BFLASH, are read and stored in computer memory--statement 1.

(2) The number of terms to be evaluated, the number of constraints on the solution, the weight function, and the reference run are all predetermined--statement 13.

(3) The solution may be constrained so that any number of the exponents may be fixed--statement 45.

(4) The log ratios are computed and stored and the Bjorck subroutine is called--statement 66 for 'weight' = 1.0 and statement 76 with weight = $(BFLASH)^2$.

(5) The exponents are returned from the Bjorck subroutine, and then BCONV, BDIF, STDDEV, MNBDIFPC, etc., are calculated--statements 16 to 20.

(6) Pertinent dimensionless numbers may be computed upon demand--statement 32.

(7) The average value of $K_{c,min}$ is computed--statement 35 + 1.

Pertinent information is printed out as it is generated, and again an option is included that permits calculation of "reference data"--statement 81. These reference conditions are derived by calling upon the Bjorck subroutine to compute a representative value of BFLASH; this value of BFLASH is derived by first evaluating the basic B-factor equation to obtain values for E1, E2, E3, etc., for a set of data. The basic B-factor equation is simply (C-1) without the parameters subscripted with "ref." Then the mean values of the physical parameters, α, V_o, etc., are computed. These mean values and the exponents, EN, are then used in the basic B-factor equation to calculate a 'representative' BFLASH--statement 85 + 8. This 'representative' BFLASH and the mean physical parameters are then used as "reference data" for the Bjorck program. This calculation method yielded low STDDEV's for comparison with those attainable using actual run data as the "reference data."

Hazards of using the Variation-of-Parameter program: Judicious selection of the initial exponent values, though not vital, helps the computer program to converge on the best solution more rapidly. The initial exponent estimates should match the anticipated results as closely as possible. Care must be taken to choose appropriate incremental steps for the exponents; if the steps are too small, a local minima may be found, and if the steps are too large, the absolute minimum may be bypassed in favor of some other minima. The number of incremental cycles should be kept to a minimum to conserve computer time and still provide appropriate bounds on the exponents. Where the physical parameter, e.g. α, does not vary much, it is wise to check for exponent convergence; i.e., be certain the exponent value is not continuously

'drifting' when the incrementing is concluded. Where the physical parameter does not vary much, the order in which the exponent is altered can drastically affect its final value, e.g., if α varies less than ten percent and E1 is the first exponent altered, weird results may be returned. Causing E1 to be the second or third exponent to be altered will normally produce much more realistic values, i.e., the exponent on a weakly varying parameter should not be one of the first to be altered. Another factor that can cause considerable confusion is the occurrence of the same physical parameter in more than one exponentiated term. As an example, it is desirable to evaluate α and kinematic viscosity, μ/ρ_o, in the same expression. Fluid density, ρ_o, is inherent in both of these terms and can interact in such a way that unpredictable results occur when both terms are used. Again, the order in which these terms are processed in the computer program may affect the outcome. Also, the initial selection of exponents can have some influence on this interaction as well as determination of the best solution.

In this program and the Bjorck program, it is wise to have some means of hand-checking the results. A crude method of doing this for our problem consists of plotting graphs as follows:

(1) Data points are selected so that only one physical parameter varies appreciably;

(2) this parameter is then plotted as the abscissa, with B/B_{ref} plotted on the ordinate of log - log graph paper;

(3) the best straight line is fitted to these plotted data; and then

(4) the slope of this line is a rough estimate of the exponent value for that particular physical parameter, see eq (C-1).

In spite of all of the drawbacks of the variation-of-parameter program, it is very useful and usually provides the lowest STDDEV and MNBDIFPC for a set of data points. Its major drawback is the computer time required, and its primary asset is the ability to provide realistic bounds for the exponents.

Hazards of using the Bjorck program: The major problem in using this program occurs where there is little variation in one or more of the physical parameters. In its present form, there are no provisions for setting realistic bounds on the exponents. The appropriate weight function must be used if minimization in the linear sense of the problem is desired. It is usually wise to run the program with and without the weight function, because minimization in the logarithmic or non-linear sense can provide superior results, i. e. , a lower value of MNBDIFPC and about the same STDDEV. This program requires little machine time and where the physical parameters vary significantly provides essentially the same results as the slower variation-of-parameter program. It serves as a good check on the slower program, because within its mathematical limitations, the absolute minimum solution is guaranteed. Because of these niceties, this program is extremely useful in correlating data from fluid-to-fluid.

Variation-of-Parameter Computer Listing

```
'JOB,2750453,HORD,4
'FTN,L,X,R
      PROGRAM BCONVECT
      DIMENSION DEL(3),RUN(405),DPM(405),DLIQ(405),VO(405),ALPHA(405),
     1LENGTH(405),DTS(405),ROVIS(405),ROSIG(405),BFLASH(405),NN(405),
     2E(5),RATIO(405,5),RATIOEXP(405,5),BCONV(405),BDIF(405),HOLD(5)
      INTEGER HOLD,REF
      REAL KCMIN,LENGTH,MNBDIFPC
      DATA (DEL=0.2,0.02,0.002)
C     THIS PROGRAM CORRELATES B-FLASH AND BCONVEC THEORIES--SIMILARITY
C     EQUATION--WITH EXPERIMENTAL DATA.
C     PROGRAM LOGIC9PROGRAM,DATA,BLANK CARD,EXPONENT-VALUE CARDS(OPTIONS
C     ),BLANK CARD,MORE DATA(E.G.DIFFERENT CAVITY LENGTHS AND PRESSURES-
C     --NN=1 TO 6),BLANK CARD, MORE EXPONENT-VALUE CARDS,THEN EOF.
C     AFTER FIRST EOF ADD AN IBRANCH CARD THAT BRANCHES INTO DIMENSION-
C     LESS NO. CALCULATION,THEN ANOTHER EOF.THE REF RUN MUST BE SPECIFIED ON
C     THE EXPONENT CARD. IF THE 4TH OR 5TH EXPONENT
C     HAS INITIAL VALUE=0.0,THAT TERM WILL BE HELD AT1.0,NOT USED,IN THE
C     SEEK-FIT OF THE OTHER EXPONENTS.THIS PROGRAM DOES FORCE-FIT INDIVIDUAL
C     TERMS .IF TERMS 1 AND 3 ARE TO BE HELD CONSTANT--TYPE 1 IN HOLD1 AND
C     3 IN HOLD3,ETC..LEAVE HOLD COLUMNS BLANK UNLESS A NON-ZERO EXPONENT
C     IS TO BE HELD CONSTANT.HOLD TERMS APPEAR ON EXPONENT CARD.
C     DECK STRUCTURE  .---DATA,BLANK CARD,EXPONENT CARDS,BLANK CARD,DATA,
C     BLANK CARD,EXPONENT CARDS,EOF,IBRANCH CARD,EOF,EOF.
C     TO OBTAIN AN IBRANCH AFTER EACH BATCH OF DATA-----DATA,BLANK CARD,
C     EXPONENT CARDS,EOF,IBRANCH CARD,MORE DATA,ETC..
   41 I=1
    1 READ 101,RUN(I),DPM(I),DLIQ(I),VO(I),ALPHA(I),LENGTH(I),DTS(I),
     1ROVIS(I),ROSIG(I),BFLASH(I),NN(I)
C     A BLANK CARD IS REQUIRED TO END DATA.
      IF(EOF,60)40,42
   42 IF(VO(I).EQ.0.0) GO TO 2
      I=I+1
      GO TO 1
    2 NPTS=I-1
C     THE FOLLOWING DO LOOP IS ELIMINATED WHEN ROSIG IS TO BE USED------
C     THIS DO LOOP IS NECESSARY TO EVALUATE SCALE EFFECTS-------WEBER NO.
C     WILL BE MEANINGLESS WHEN THIS DO LOOP IS USED
      DO 44  I=1,NPTS
      ROSIG(I)=DTS(I)
   44 CONTINUE
    3 READ 102,(E(I),I=1,5),(HOLD(I),I=1,5),REF
C     IF REF =1 THE FIRST CARD READ WILL BE USED AS REF RUN,IF REF=10 THE 10TH
C     CARD WILL BE USED,IF REF=0 THE REF RUN WILL BE CALCULATED AND REF WILL
C     BE SET EQUAL TO NPTS+1.
      IF(EOF,60)30,21
   21 IF(E(1).EQ.0.0) GO TO 41
      IF(REF.EQ.0.0)51,24
   24 IF(E(4).EQ.0.0)6,5
    4 LIM=3
      GO TO 9
    5 IF(E(5).EQ.0.0) GO TO 7
      GO TO 8
C     6+1 STARTS CALC FOR FIRST 3 AND 5TH TERMS


71 08 05

70
```

```
    6 IF(E(5).EQ.0.0) GO TO 4
      LIM=5
      DO 22  I=1,NPTS
      RATIO(I,1)=ALPHA(REF)/ALPHA(I)
      RATIO(I,2)=VO(I)/VO(REF)
      RATIO(I,3)=LENGTH(I)/LENGTH(REF)
      RATIO(I,4)=1.0
      RATIO(I,5)=ROSIG(I)/ROSIG(REF)
   22 CONTINUE
      GO TO 23
    7 LIM=4
      GO TO 9
    8 LIM=5
      GO TO 9
C     STATEMENT 9 STARTS CALCULATION FOR FIRST 3,4, OR ALL 5 TERMS OF EQUATION.
    9 DO 10  I=1,NPTS
      RATIO(I,1)=ALPHA(REF)/ALPHA(I)
      RATIO(I,2)=VO(I)/VO(REF)
      RATIO(I,3)=LENGTH(I)/LENGTH(REF)
      RATIO(I,4)=ROVIS(I)/ROVIS(REF)
      RATIO(I,5)=ROSIG(I)/ROSIG(REF)
   10 CONTINUE
   23 DO 11  I=1,NPTS
      DO 11  J=1,LIM
      RATIOEXP(I,J)=RATIO(I,J)**E(J)
   11 CONTINUE
      MJ=LIM
      DO 18  MM=1,3
      DO 18  K=1,20
      DO 18  J=1,MJ
      IF(HOLD(J).EQ.J) GO TO 18
      SUMBDIF=0.0
      DO 13  I=1,NPTS
      BCONV(I)=BFLASH(REF)
      DO 12  JJ=1,LIM
      BCONV(I)=BCONV(I)*RATIOEXP(I,JJ)
   12 CONTINUE
      BDIF(I)=BCONV(I)-BFLASH(I)
      SUMBDIF=SUMBDIF+BDIF(I)*BDIF(I)
   13 CONTINUE
      WRITE(61,103)(E(I),I=1,5),SUMBDIF
      RESIDUE=0.0
      DO 14  I=1,NPTS
      EE=RATIO(I,J)
      RESIDUE=RESIDUE+BDIF(I)*LOGF(EE)*BCONV(I)
   14 CONTINUE
      IF(RESIDUE)15,18,16
   15 E(J)=E(J)+DEL(MM)
      GO TO 17
   16 E(J)=E(J)-DEL(MM)
   17 CONTINUE
      DO 18  I=1,NPTS
      RATIOEXP(I,J)=RATIO(I,J)**E(J)
   18 CONTINUE


71 08 05
```

```
      WRITE(61,104)
      SUMBDIF=0.0
      SMBDIFPC=0.0
      DO 20  I=1,NPTS
      BCONV(I)=BFLASH(REF)
      DO 19  JJ=1,LIM
      BCONV(I)=BCONV(I)*RATIOEXP(I,JJ)
   19 CONTINUE
      BDIF(I)=BCONV(I)-BFLASH(I)
      BDIFPC=(BDIF(I)/BFLASH(I))*100.0
      SMBDIFPC=SMBDIFPC+ABSF(BDIFPC)
      SUMBDIF=SUMBDIF+BDIF(I)*BDIF(I)
      WRITE(61,105)RUN(I),ALPHA(I),VO(I),LENGTH(I),ROVIS(I),ROSIG(I),
     1BCONV(I),BFLASH(I),BDIF(I),BDIFPC,SUMBDIF,DTS(I),NN(I)
C     BDIFPC=PERCENTAGE BDIF AND SUMBDIF=SUMMATION OF BDIF SQUARED
   20 CONTINUE
      IF(REF.GT.NPTS) GO TO 26
      STDDEV=SQRTF(SUMBDIF/(NPTS-1))
      GO TO 27
   26 STDDEV=SQRTF(SUMBDIF/NPTS)
   27 WRITE(61,106)(E(I),I=1,5),STDDEV
      WRITE(61,111)RUN(REF)
      MNBDIFPC=SMBDIFPC/(NPTS-1)
      WRITE(61,112)MNBDIFPC
      GO TO 3
   51 REF=NPTS+1
      ALPHA(REF)=0.0
      VO(REF)=0.0
      LENGTH(REF)=0.0
      ROVIS(REF)=0.0
      ROSIG(REF)=0.0
      BFLASH(REF)=0.0
      DO 55  I=1,NPTS
      ALPHA(REF)=ALPHA(REF)+ALPHA(I)
      VO(REF)=VO(REF)+VO(I)
      LENGTH(REF)=LENGTH(REF)+LENGTH(I)
      ROVIS(REF)=ROVIS(REF)+ROVIS(I)
      ROSIG(REF)=ROSIG(REF)+ROSIG(I)
      BFLASH(REF)=BFLASH(REF)+BFLASH(I)
   55 CONTINUE
      ALPHA(REF)=ALPHA(REF)/NPTS
      VO(REF)=VO(REF)/NPTS
      LENGTH(REF)=LENGTH(REF)/NPTS
      ROVIS(REF)=ROVIS(REF)/NPTS
      ROSIG(REF)=ROSIG(REF)/NPTS
      BFLASH(REF)=BFLASH(REF)/NPTS
      RUN(REF)=99999
      DPM(REF)=1.
      GO TO 24
C     IF IBRANCH EQUALS ZERO--DIMENSIONLESS NOS ARE RETURNED
   30 READ 107,IBRANCH
      IF(EOF,60)40,31
   31 IF(IBRANCH.EQ.0.0) GO TO 32
      GO TO 30


   71 08 05
```

```
   32 WRITE(61,108)
      SUMKCMIN=0.0
C     THIS PROGRAM HAS THE OPTION OF USING REF RUN DATA CALCULATED IN
C     THE BJORCK PROGRAM--------.
C     CALC REF RUN DATA CARD (FROM BJORCK PROGRAM) SHOULD BE LAST DATA CARD IN
C     DATA DECK
      IF(DPM(REF).EQ.0.0)34,33
   34 NPTS=NPTS-1
   33 DO 35  I=1,NPTS
      KCMIN=2.306658726*2.0*32.1725*DPM(I)/(DLIQ(I)*VO(I)**2.0)
      SUMKCMIN=SUMKCMIN+KCMIN
      PRANDTL=1.0/(ALPHA(I)*ROVIS(I))
      RED=77.4192*ROVIS(I)*VO(I)*DTS(I)
      REX=77.4192*ROVIS(I)*VO(I)*LENGTH(I)
      FROUDE=VO(I)/SQRTF(LENGTH(I)*2.68104)
      WEBER=2359.737216*ROSIG(I)*LENGTH(I)*VO(I)**2.0
      PECLET=PRANDTL*RED
      WRITE(61,109)RUN(I),ALPHA(I),VO(I),LENGTH(I),ROVIS(I),ROSIG(I),
     1DTS(I),KCMIN,PRANDTL,RED,REX,FROUDE,WEBER,PECLET
   35 CONTINUE
      AVGKCMIN=SUMKCMIN/NPTS
      WRITE(61,110)AVGKCMIN
      GO TO 41
  101 FORMAT(A5,2F7.4,F8.3,E11.4,2F6.3,E11.4,F8.5,F8.4,2X,I1)
  102 FORMAT(5(F10.4),6(I5))
  103 FORMAT(* E1= *,F8.3,5X,*E2=*,F8.3,5X,*E3=*,F8.3,5X,*E4=*,F8.3,
     15X,*E5=*,F8.3,5X,*SUMBDIFSQ=*,E15.5)
  104 FORMAT(*1RUN*,5X,*ALPHA*,6X,*VO*,3X,*LENGTH*,6X,*ROVIS*,3X,*ROSIG*
     1,3X,*BCONV*,2X,*BFLASH*,4X,*BDIF*,2X,*BDIFPC*,5X,*SUMBDIFSQ*,6X,
     2*DTS*,9X,*NN*,//)
  105 FORMAT(A5,E11.4,F8.3,F7.3,E11.4,F8.5,F8.4,F8.4,F8.4,F8.1,E16.5,
     1 F8.4,9X,I1)
  106 FORMAT(///,2X,*E1=*,F8.3,5X,*E2=*,F8.3,5X,*E3=*,F8.3,5X,*E4=*,F8.3
     1,5X,*E5=*,F8.3,10X,*STDDEV=*,F10.4)
  107 FORMAT(I1)
  108 FORMAT(*1RUN*,5X,*ALPHA*,6X,*VO*,3X,*LENGTH*,6X,*ROVIS*,3X,*ROSIG*
     1,5X,*DTS*,3X,*KCMIN*,4X,*PR*,6X,*RED*,10X,*REX*,8X,*FR*,9X,*WE*,
     27X,*PECLET*,//)
  109 FORMAT(A5,E11.4,F8.3,F7.3,E11.4,F8.5,F8.4,F8.3,F8.3,E12.2,E12.2,F
     18.2,E12.2,E12.2)
  110 FORMAT(///,2X,*AVGKCMIN=*,F8.3,8(/))
  111 FORMAT(///,9X,*REF RUN=*,A5,2(/))
  112 FORMAT(8X,*MNBDIFPC=*,F7.1,8(/))
   40 CALL EXIT
      END
         SCOPE
'LOAD
'RUN,4,10000,7
```

71 08 05

```
!JOB,2750453,HORD J,2
!FTN,L,X,R
      PROGRAM BCONVECT
      DIMENSION RUN(405),DPM(405),DLIQ(405),VO(405),ALPHA(405),LENGTH
     1 (405),DTS(405), ROVIS(405), ROSIG(405),BFLASH(405),NN(405),E(5)
      COMMON M1,M,N,A(410,6),B(410),W(410),X(7),RES(410),V(6,6),STD
      REAL KCMIN,LENGTH,MNBDIFPC
      INTEGER TERM1,TERM2,TERM3,TERM4,TERM5,WGHT,REF
C     THIS PROGRAM CORRELATES B-FLASH AND BCONVEC THEORIES-- SIMILARITY
C     EQUATION-- WITH EXPERIMENTAL DATA.
C     PROGRAM LOGIC9(WITH BJORCK)---DATA,EOF,NF CARD,NF CARD,NF CARD
C     ETC.,EOF,DATA,EOF,NF CARDS,EOF,,EOF.(TAKES 2EOFS TOTERMINATE
C     PROGRAM.)FOR FORCE FIT ADD AN EXTRA CARD AFTER NF CARD--THIS CARD
C     WILL DEFINE THE TERM TO BE FIXED AND ITS EXPONENT VALUE. THIS CARD
C     IS REQUIRED ONLY IF M1 GREATER THAN 0.FOR EXAMPLE TO FORCE-FIT THE
C     1,2ND,AND5TH TERMS WITH EXPONENTS OF .6,0.5, AND 0.4,--TYPE THE
C     TERM CARD AS FOLLOWS9 TERM1=1,TERM2=2,TERM3=5,LEAVE TERM4 AND
C     TERM5 BLANK AND TYPE E1=0.6,E2=0.5 AND E3=0.4,LEAVE E4 ANDE5 BLANK
C     I.E.,THE E(I) MUST MATCH THE TERM BEING HELD CONSTANT. USE M1=0
C     FOR NO CONSTRAINTS AND THE TERM CARD IS NOT REQUIRED FOR A 3, 4,
C     OR 5 TERM FIT(ALL EXPONENTS ARE JUGGLED). TO FORCE-FIT THE 3D TERM
C     WITH EXPONENT=0.5,SETM1=1 ON NF CARD THEN TYPE THE TERM CARD TERM1
C     =3 AND E1=0.5, ETC..
   41 I=1
    1 READ 101 ,RUN(I),DPM(I),DLIQ(I),VO(I),ALPHA(I),LENGTH(I),DTS(I),
     1ROVIS(I),ROSIG(I),BFLASH(I),NN(I)
      IF(EOF,60)4,2
    2 I=I+1
      GO TO 1
    4 NPTS=I-1
      IF(NPTS.EQ.0.0) GO TO 40
      M=NPTS
C     THE FOLLOWING DO LOOP SHOULD BE ELIMINATED WHEN ROSIG IS TO BE USED
C     THIS DO LOOP IS NECESSARY TO EVALUATE SCALE EFFECTS--------
C     WEBER NO. WILL BE MEANINGLESS WHEN THIS DO LOOP IS USED.
      DO 44  I=1,NPTS
      ROSIG(I)=DTS(I)
   44 CONTINUE
C     IF WGHT=1,W(I)=1 AND IF WGHT=2, W(I)=BFLASH(I)*BFLASH(I)
   13 READ 110,NF,M1,IBRANCH,WGHT,REF
C     IF REF =1 THE FIRST CARD READ WILL BE USED AS REF RUN,IF REF=10 THE 10TH
C     CARD WILL BE USED,IF REF=0 THE REF RUN WILL BE CALCULATED AND REF WILL
C     BE SET EQUAL TO NPTS+1.
      IF(EOF,60)41,65
   65 IF(REF.EQ.0.0)81,5
    5 N=NF
      IF(M1.GT.0.0) GO TO 45
    6 GO TO (66,76),WGHT
   66 DO 8  I=1,M
      B(I+M1)=LOGF(BFLASH(I)/BFLASH(REF))
    7 A(I+M1,1)=LOGF(ALPHA(REF)/ALPHA(I))
      A(I+M1,2)=LOGF(VO(I)/VO(REF))
      A(I+M1,3)=LOGF(LENGTH(I)/LENGTH(REF))
      A(I+M1,4)=LOGF(ROVIS(I)/ROVIS(REF))


71 08 05
```

```
      A(I+M1,5)=LOGF(ROSIG(I)/ROSIG(REF))
    8 CONTINUE
      CALL BJORCK
      PRINT 112
   12 DO 10  I=1,M
      JIM=I+M1
   10 PRINT 102,RUN(I),RES(JIM)
   11 PRINT 103,(X(J),J=1,NF)
      PRINT 107,STD
   14 PRINT 104,NF
C     LOGF(BCONV(I)/BFLASH(REF))=ZZ
      SUMBDIF=0.0
      SMBDIFPC=0.0
      DO 18  I=1,M
      ZZ=0.0
      DO 16  J=1,NF
   16 ZZ=ZZ+A(I+M1,J)*X(J)
      BCONV=BFLASH(REF)*EXPF(ZZ)
      BDIF=BCONV-BFLASH(I)
      BDIFPC=(BDIF/BFLASH(I))*100.0
      SMBDIFPC=SMBDIFPC+ABSF(BDIFPC)
      SUMBDIF=SUMBDIF+BDIF*BDIF
      WRITE(61,105)RUN(I),ALPHA(I),VO(I),LENGTH(I),ROVIS(I),ROSIG(I),
     1BCONV    ,BFLASH(I),BDIF    ,BDIFPC,SUMBDIF,DTS(I),NN(I)
   18 CONTINUE
      IF(REF.GT.NPTS) GO TO 20
      STDDEV=SQRTF(SUMBDIF/(NPTS-1))
      MNBDIFPC=SMBDIFPC/(NPTS-1)
      GO TO 21
   20 STDDEV=SQRTF(SUMBDIF/NPTS)
      MNBDIFPC=SMBDIFPC/(NPTS)
   21 WRITE(61,106)STDDEV
      WRITE(61,114)RUN(REF),WGHT,MNBDIFPC
C     IF IBRANCH EQUALS ZERO--DIMENSIONLESS NOS ARE RETURNED
      IF(IBRANCH.EQ.0.0) GO TO 32
      GO TO 13
C     A TERM AND EXPONENT CARD MUST FOLLOW ALL NF CARDS WHERE M1 .GT.0.
   45 READ 111,TERM1,TERM2,TERM3,TERM4,TERM5,(E(I),I=1,M1)
      IF(EOF,60)40,47
   47 DO 60  K=1,M1
      GO TO (51,52,53,54,55),K
   51 KK=TERM1
      GO TO 57
   52 KK=TERM2
      GO TO 57
   53 KK=TERM3
      GO TO 57
   54 KK=TERM4
      GO TO 57
   55 KK=TERM5
      GO TO 57
   57 B(K)=E(K)
      A(K,KK)=1.0
      KIM=KK-1


71 08 05
```

```
      KIMN=KK+1
      DO 58  L=1,KIM
      A(K,L)=0.0
   58 CONTINUE
      DO 59  L=KIMN,NF
      A(K,L)=0.0
   59 CONTINUE
   60 CONTINUE
      GO TO 6
   76 DO 78  I=1,M
      B(I+M1)=LOGF(BFLASH(I)/BFLASH(REF))
   77 A(I+M1,1)=LOGF(ALPHA(REF)/ALPHA(I))
      A(I+M1,2)=LOGF(VO(I)/VO(REF))
      A(I+M1,3)=LOGF(LENGTH(I)/LENGTH(REF))
      A(I+M1,4)=LOGF(ROVIS(I)/ROVIS(REF))
      A(I+M1,5)=LOGF(ROSIG(I)/ROSIG(REF))
C     W(I+M1)=THE WEIGHT REQUIRED FOR LEAST SQUARES MINIMIZATION ON THE
C     LINEAR PROBLEM----NOT MINIMIZATION IN THE LOGARITHMIC SENSE
C     MINIMIZING IN THE LOG SENSE IS DONE ON BDIFPC*BDIFPC(WHEN WGHT=1)
      W(I+M1)=BFLASH(I)*BFLASH(I)
   78 CONTINUE
      CALL WEIGHT
      PRINT 112
      GO TO 12
C     STATEMENT 81 STARTS CALC OF REF CONDITIONS USING BASIC BCONV EQUATION
   81 ISETM1=M1
      M1=0.
      N=6
      DO 82  I=1,NPTS
      B(I)=LOGF(BFLASH(I))
      A(I,1)=1.0
      A(I,2)=LOGF(ALPHA(I))
      A(I,3)=LOGF(VO(I))
      A(I,4)=LOGF(LENGTH(I))
      A(I,5)=LOGF(ROVIS(I))
      A(I,6)=LOGF(ROSIG(I))
   82 CONTINUE
      CALL BJORCK
   83 REF=NPTS+1
      ALPHA(REF)=0.0
      VO(REF)=0.0
      LENGTH(REF)=0.0
      ROVIS(REF)=0.0
      ROSIG(REF)=0.0
      DO 85  I=1,NPTS
      ALPHA(REF)=ALPHA(REF)+ALPHA(I)
      VO(REF)=VO(REF)+VO(I)
      LENGTH(REF)=LENGTH(REF)+LENGTH(I)
      ROVIS(REF)=ROVIS(REF)+ROVIS(I)
      ROSIG(REF)=ROSIG(REF)+ROSIG(I)
   85 CONTINUE
      ALPHA(REF)=ALPHA(REF)/NPTS
      VO(REF)=VO(REF)/NPTS
      LENGTH(REF)=LENGTH(REF)/NPTS


71 08 05
```

```
      ROVIS(REF)=ROVIS(REF)/NPTS
      ROSIG(REF)=ROSIG(REF)/NPTS
      PP=X(1)+X(2)*LOGF(ALPHA(REF))+X(3)*LOGF(VO(REF))+X(4)*LOGF(LENGTH
     1 (REF))+X(5)*LOGF(ROVIS(REF))+X(6)*LOGF(ROSIG(REF))
      BFLASH(REF)=EXPF(PP)
      M1=ISETM1
      RUN(REF)=99999
      DPM(REF)=0.0
      DLIQ(REF)=0.0
      DTS(REF)=DTS(1)
      NN(REF)=NN(1)
      PRINT 115,BFLASH(REF),ALPHA(REF),VO(REF),LENGTH(REF),ROVIS(REF),
     1 ROSIG(REF)
C     A PUNCH STATEMENT IDENTICAL TO PRINT 115 SUPPLIES THIS CALCULATED
C     REF DATA TO VARIATION-OF-PARAMETER PROGRAM
      GO TO 5
   32 WRITE(61,108)
      SUMKCMIN=0.0
   33 DO 35  I=1,NPTS
      KCMIN=2.306658726*2.0*32.1725*DPM(I)/(DLIQ(I)*VO(I)**2.0)
      SUMKCMIN=SUMKCMIN+KCMIN
      PRANDTL=1.0/(ALPHA(I)*ROVIS(I))
      RED=77.4192*ROVIS(I)*VO(I)*DTS(I)
      REX=77.4192*ROVIS(I)*VO(I)*LENGTH(I)
      FROUDE=VO(I)/SQRTF(LENGTH(I)*2.68104)
      WEBER=2359.737216*ROSIG(I)*LENGTH(I)*VO(I)**2.0
      PECLET=PRANDTL*RED
      WRITE(61,109)RUN(I),ALPHA(I),VO(I),LENGTH(I),ROVIS(I),ROSIG(I),
     1DTS(I),KCMIN,PRANDTL,RED,REX,FROUDE,WEBER,PECLET
   35 CONTINUE
      AVGKCMIN=SUMKCMIN/NPTS
      WRITE(61,113)AVGKCMIN
  101 FORMAT(A5,2F7.4,F8.3,E11.4,2F6.3,E11.4,F8.5,F8.4,2X,I1)
  102 FORMAT(A5,E20.5)
  103 FORMAT(*1 ZZ IS THE SUM OF THE FOLLOWING TERMS9*//*0 ZZ=*E17.10,
     1 8H*A(I, 1)E17.10,8H*A(I, 2)E17.10,8H*A(I, 3)
     2 /*0*E17.10,8H*A(I, 4)E17.10,8H*A(I, 5)E17.10,8H*A(I, 6))
  104 FORMAT(*1*,I1,* FUNCTIONS GIVES THE FOLLOWING FIT9*///*RUN*,5X,
     1*ALPHA*,6X,*VO*,3X,*LENGTH*,6X,*ROVIS*,3X,*ROSIG*,3X,*BCONV*,2X,
     2 *BFLASH*,4X,*BDIF*,2X,*BDIFPC*,5X,*SUMBDIFSQ*,6X,*DTS*,9X,*NN*//)
  105 FORMAT(A5,E11.4,F8.3,F7.3,E11.4,F8.5,F8.4,F8.4,F8.4,F8.1,E16.5,
     1 F8.4,9X,I1)
  106 FORMAT(////,*STD DEVIATION AS COMPUTED BY SUMBDIFSQ=*,F10.5)
  107 FORMAT(*0STD DEV OF THE FIT=*,F10.5)
  108 FORMAT(*1RUN*,5X,*ALPHA*,6X,*VO*,3X,*LENGTH*,6X,*ROVIS*,3X,*ROSIG*
     1,5X,*DTS*,3X,*KCMIN*,4X,*PR*,6X,*RED*,10X,*REX*,8X,*FR*,9X,*WE*,
     27X,*PECLET*,//)
  109 FORMAT(A5,E11.4,F8.3,F7.3,E11.4,F8.5,F8.4,F8.3,F8.3,E12.2,E12.2,F
     18.2,E12.2,E12.2)
  110 FORMAT(5(I5))
  111 FORMAT(5(I5),5(F10.3))
  112 FORMAT(*1RUN*,15X,*RES*,//)
  113 FORMAT(///,2X,*AVGKCMIN=*,F8.3)
  114 FORMAT(///,2X,* REF RUN=*,A5,20X,*WGHT=*,I5,20X,*MNBDIFPC=*,F7.1
```

71 08 05

```
     1,6(/))
  115 FORMAT(*CALC BFLASH(REF)=*,F8.4,/,*CALC ALPHA(REF)=*,E11.4,/,*CALC
     1VO(REF)=*,F8.3,/,*CALC LENGTH(REF)=*,F7.3,/,*CALC ROVIS(REF)=*,
     2 E11.4,/,*CALC ROSIG(REF)=*,F8.5,6(/))
   40 CALL EXIT
      END
      SUBROUTINE BJORCK                                                  BJOR001
      DIMENSION Q(410,6),G(6),F(410),Y(6),D(6),NPV(6),P(7),SW(410)
      COMMON M1,M,N,A(410,6),B(410),W(410),X(7),RES(410),V(6,6),STD
C                                                                        BJOR004
C         THE FOLLOWING VALUES MUST BE SET BEFORE THE CALL               BJOR005
C         A(I,J) = THE  J  FUNCTION EVALUATED AT THE  I  POINT           BJOR006
C         B(I) = THE VALUE OF THE  I  ORDINATE                           BJOR007
C         W(I) = THE WEIGHT TO BE APPLIED TO THE  I  POINT               BJOR008
C         M = THE NUMBER OF POINTS  ( I )                                BJOR009
C         N = THE NUMBER OF FUNCTIONS  ( J )                             BJOR010
C         M1 = THE NUMBER OF ROWS IN A THAT MUST BE SATISFIED EXACTLY    BJOR011
C             (NUMBER OF CONSTRAINTS)                                    BJOR012
C                                                                        BJOR013
C         AFTER THE CALL                                                 BJOR014
C         X(J) = THE MEAN-LEAST-SQUARE COEFFICIENT OF THE  J  FUNCTION   BJOR015
C         RES(I) = THE MEAN LEAST SQUARE DEVIATION OF THE  I  POINT      BJOR016
C         V(I,J) = THE VARIANCE - COVARIANCE MATRIX                      BJOR017
C         STD = THE STANDARD DEVIATION OF THE FIT                        BJOR018
C                                                                        BJOR019
C         THE METHOD IS THAT OF AKE BJORCK, AS DESCRIBED IN              BJOR020
C         NORDISK TIDSKRIFT FOR INFORMATIONS-BEHANDLING                  BJOR021
C          BIT  VOL.7, PP.257-278 (1967) AND VOL.8, PP.8-30 (1968)       BJOR022
C                                                                        BJOR023
C         THE WEIGHTING OF EACH POINT IS 1.0 UNLESS THE ENTRY  WEIGHT    BJOR024
C         IS USED.                                                       BJOR025
C                                                                        BJOR026
C         THE SUBROUTINE  ACPROD(A,B,N,C)  SUMS THE FIRST N PRODUCTS OF  BJOR027
C         A(I)*B(I) AND ADDS C IN DOUBLE THE OPERATING PRECISION AND IS, BJOR028
C         THEREFORE, MACHINE DEPENDENT.  THE OPERATING PRECISION IS      BJOR029
C         DEFINED BY THE VALUE OF  ETA  WHICH IS 1/2 RAISED TO A POWER   BJOR030
C         EQUAL TO THE NUMBER OF BITS CARRIED IN THE ARITHMETIC          BJOR031
C         OPERATIONS (IN THIS CASE, 36)                                  BJOR032
C                                                                        BJOR033
      DATA (ETA=1.45519152284E-11)                                       BJOR034
      DO 10 I=1,M                                                        BJOR035
   10 SW(I)=1.                                                           BJOR036
   11 ETA2=ETA*ETA                                                       BJOR037
      C=36*N                                                             BJOR038
      TOL2=C*ETA2                                                        BJOR039
      MP=M1+1                                                            BJOR040
      DO 13 J=1,N                                                        BJOR041
      NPV(J)=J                                                           BJOR042
      DO 12 I=1,N                                                        BJOR043
   12 V(I,J)=0.                                                          BJOR044
      DO 13 I=1,M                                                        BJOR045
   13 Q(I,J)=A(I,J)*SW(I)                                                BJOR046
      MV=1                                                               BJOR047
      MH=M1                                                              BJOR048
```

71 08 05

```
      NTR=1                                                          BJOR049
      DO 30 K=1,N                                                    BJOR050
      NP=K                                                           BJOR051
      IF(K.NE.MP) GO TO 15                                           BJOR052
      MV=MP                                                          BJOR053
      MH=M                                                           BJOR054
   14 NTR=1                                                          BJOR055
   15 DS=0.                                                          BJOR056
      DO 20 J=K,N                                                    BJOR057
      L=NPV(J)                                                       BJOR058
      IF(NTR.EQ.0) GO TO 17                                          BJOR059
      D(J)=0.                                                        BJOR060
      DO 16 I=MV,MH                                                  BJOR061
   16 D(J)=D(J)+Q(I,L)*Q(I,L)                                        BJOR062
   17 IF(DS.GE.D(J)) GO TO 20                                        BJOR063
      DS=D(J)                                                        BJOR064
      NP=J                                                           BJOR065
   20 CONTINUE                                                       BJOR066
      L=NPV(NP)                                                      BJOR067
      IF(NTR.EQ.1) DM=DS                                             BJOR068
      NTR=0                                                          BJOR069
      IF(DS.LT.ETA*DM) GO TO 14                                      BJOR070
      IF(NP.EQ.K) GO TO 22                                           BJOR071
      D(NP)=D(K)                                                     BJOR072
      NPV(NP)=NPV(K)                                                 BJOR073
      NPV(K)=L                                                       BJOR074
      KM=K-1                                                         BJOR075
      DO 21 I=1,KM                                                   BJOR076
      C=V(I,NP)                                                      BJOR077
      V(I,NP)=V(I,K)                                                 BJOR078
   21 V(I,K)=C                                                       BJOR079
   22 DS=0.                                                          BJOR080
      DO 23 I=MV,MH                                                  BJOR081
   23 DS=DS+Q(I,L)*Q(I,L)                                            BJOR082
      D(K)=DS                                                        BJOR083
      IF(K.LE.M1) GO TO 24                                           BJOR084
      IF(DS.LE.TOL2*D(MP)*V(MP,K)*V(MP,K)) GO TO 31                  BJOR085
   24 IF(DS.LE.0.) GO TO 44                                          BJOR086
      KM=K+1                                                         BJOR087
      IF(KM.GT.N) GO TO 30                                           BJOR088
      DO 27 J=KM,N                                                   BJOR089
      NP=NPV(J)                                                      BJOR090
      DO 25 I=MV,MH                                                  BJOR091
   25 V(K,J)=V(K,J)+Q(I,L)*Q(I,NP)                                   BJOR092
      V(K,J)=V(K,J)/DS                                               BJOR093
      DO 26 I=MV,M                                                   BJOR094
   26 Q(I,NP)=Q(I,NP)-V(K,J)*Q(I,L)                                  BJOR095
   27 D(J)=D(J)-DS*V(K,J)*V(K,J)                                     BJOR096
   30 N1=K                                                           BJOR097
   31 DS=1.                                                          BJOR098
   33 STD=0.                                                         BJOR099
      DO 35 I=1,M                                                    BJOR100
      RES(I)=0.                                                      BJOR101
   35 F(I)=B(I)*SW(I)                                                BJOR102


71 08 05
```

```
      DO 37 J=1,N                                                          BJOR103
      X(J)=0.                                                              BJOR104
   37 G(J)=0.                                                              BJOR105
      X(N+1)=-1.                                                           BJOR106
      ITER=-1                                                              BJOR107
      IF(DS.GT.0.) GO TO 55                                                BJOR108
      DO 39 J=1,N                                                          BJOR109
      DO 39 I=1,M1                                                         BJOR110
   39 V(I,J)=0.                                                            BJOR111
      RETURN                                                               BJOR112
   40 FORMAT(120H0$$$$$$ AT LEAST TWO OF THE CONSTRAINTS ARE EQUIVALENT.BJOR113
     1  FITTING WAS TERMINATED AND ALL COEFFICIENTS SET TO ZERO $$$$$$$)BJOR114
   41 FORMAT(120H0$$$$$$$$$$$$$$$$$$$$$$$$$$$$$$$$$$$$$$$$$$$$ ITERATION FAILBJOR115
     1S TO IMPROVE THE SOLUTION $$$$$$$$$$$$$$$$$$$$$$$$$$$$$$$$$$$$$$$$)BJOR116
      ENTRY WEIGHT                                                         BJOR117
      DO 43 I=1,M                                                          BJOR118
      IF(W(I).LT.0.) W(I)=0.                                               BJOR119
   43 SW(I)=SQRT(W(I))                                                     BJOR120
      GO TO 11                                                             BJOR121
   44 PRINT 40                                                             BJOR122
      GO TO 33                                                             BJOR123
   45 DO 46 I=1,M                                                          BJOR124
   46 RES(I)=RES(I)+F(I)                                                   BJOR125
      DO 47 K=1,N1                                                         BJOR126
      J=NPV(K)                                                             BJOR127
   47 X(J)=X(J)+G(K)                                                       BJOR128
      IF(DX2.LT.ETA2*X1) GO TO 70                                          BJOR129
      IF(DR2.LT.ETA2*R1) GO TO 70                                          BJOR130
      IF(64.D0*DX2.LT.DX1) GO TO 50                                        BJOR131
      IF(64.D0*DR2.LT.DR1) GO TO 50                                        BJOR132
      PRINT 41                                                             BJOR133
      GO TO 70                                                             BJOR134
   50 DX1=DX2                                                              BJOR135
      DR1=DR2                                                              BJOR136
      DO 52 K=1,N1                                                         BJOR137
      J=NPV(K)                                                             BJOR138
      DO 51 I=1,M                                                          BJOR139
   51 F(I)=A(I,J)*SW(I)                                                    BJOR140
   52 G(K)=-ACPROD(F,RES,M,0.)                                             BJOR141
      C=0.                                                                 BJOR142
      DO 54 I=1,M                                                          BJOR143
      DO 53 J=1,N                                                          BJOR144
   53 P(J)=A(I,J)*SW(I)                                                    BJOR145
      P(N+1)=B(I)*SW(I)                                                    BJOR146
      IF(I.GT.M1) C=RES(I)                                                 BJOR147
   54 F(I)=-ACPROD(P,X,N+1,C)                                              BJOR148
   55 MV=1                                                                 BJOR149
      MH=M1                                                                BJOR150
      DO 60 K=1,N1                                                         BJOR151
      J=NPV(K)                                                             BJOR152
      IF(K.NE.MP) GO TO 56                                                 BJOR153
      MV=MP                                                                BJOR154
      MH=M                                                                 BJOR155
   56 Y(K)=G(K)                                                            BJOR156


71 08 05
```

```
      IF(K.EQ.1) GO TO 58                                          BJOR157
      L=K-1                                                        BJOR158
      DO 57 I=1,L                                                  BJOR159
   57 Y(K)=Y(K)-V(I,K)*Y(I)                                        BJOR160
   58 G(K)=0.                                                      BJOR161
      IF(K.GT.M1) G(K)=-Y(K)                                       BJOR162
      DO 59 I=MV,MH                                                BJOR163
   59 G(K)=G(K)+Q(I,J)*F(I)                                        BJOR164
      G(K)=G(K)/D(K)                                               BJOR165
      DO 60 I=MV,M                                                 BJOR166
   60 F(I)=F(I)-G(K)*Q(I,J)                                        BJOR167
      IF(M1.LE.0) GO TO 65                                         BJOR168
      DO 62 I=1,M1                                                 BJOR169
   62 F(I)=0.                                                      BJOR170
      DO 64 K=1,M1                                                 BJOR171
      J=NPV(K)                                                     BJOR172
      C=0.                                                         BJOR173
      DO 63 I=1,M                                                  BJOR174
   63 C=C+Q(I,J)*F(I)                                              BJOR175
      C=(C-Y(K))/D(K)                                              BJOR176
      DO 64 I=1,M1                                                 BJOR177
   64 F(I)=F(I)-C*Q(I,J)                                           BJOR178
   65 DO 67 LL=2,N1                                                BJOR179
      K=N1-LL+1                                                    BJOR180
      L=K+1                                                        BJOR181
      DO 66 I=L,N1                                                 BJOR182
   66 G(K)=G(K)-V(K,I)*G(I)                                        BJOR183
   67 CONTINUE                                                     BJOR184
      DX2=0.                                                       BJOR185
      DO 68 K=1,N1                                                 BJOR186
   68 DX2=DX2+G(K)*G(K)                                            BJOR187
      DR2=0.                                                       BJOR188
      DO 69 I=1,M                                                  BJOR189
   69 DR2=DR2+F(I)*F(I)                                            BJOR190
      ITER=ITER+1                                                  BJOR191
      IF(ITER.GT.0) GO TO 45                                       BJOR192
      X1=DX2                                                       BJOR193
      R1=DR2                                                       BJOR194
      DX1=X1*65.                                                   BJOR195
      GO TO 45                                                     BJOR196
   70 NRP=0                                                        BJOR197
      DO 73 I=1,M                                                  BJOR198
      IF(I.LE.M1) SW(I)=0.                                         BJOR199
      IF(SW(I).GT.0.) GO TO 72                                     BJOR200
      DO 71 J=1,N                                                  BJOR201
   71 P(J)=A(I,J)                                                  BJOR202
      P(N+1)=B(I)                                                  BJOR203
      RES(I)=-ACPROD(P,X,N+1,0.)                                   BJOR204
      GO TO 73                                                     BJOR205
   72 NRP=NRP+1                                                    BJOR206
      STD=STD+RES(I)*RES(I)                                        BJOR207
      RES(I)=RES(I)/SW(I)                                          BJOR208
   73 CONTINUE                                                     BJOR209
      I=M1+NRP-N1                                                  BJOR210


71 08 05
```

```
      IF(I.GT.0) GO TO 74                                                BJOR211
      DS=0.                                                              BJOR212
      GO TO 75                                                           BJOR213
   74 DS=STD/I                                                           BJOR214
   75 STD=SQRT(DS)                                                       BJOR215
      L=N1                                                               BJOR216
      IF(L.GT.M1) V(L,L)=1./D(L)                                         BJOR217
      IF(N1.GE.N) GO TO 77                                               BJOR218
      DO 76 I=N1,N                                                       BJOR219
   76 V(L,I)=0.                                                          BJOR220
   77 J=L-1                                                              BJOR221
      IF(J.GT.M1) V(J,J)=1./D(J)                                         BJOR222
      DO 78 K=L,N1                                                       BJOR223
   78 P(K)=V(J,K)                                                        BJOR224
      I=N1                                                               BJOR225
      DO 80 KA=J,N                                                       BJOR226
      DO 79 K=L,N                                                        BJOR227
   79 V(I,J)=V(I,J)-P(K)*V(K,I)                                          BJOR228
   80 I=I-1                                                              BJOR229
      DO 81 K=L,N                                                        BJOR230
   81 V(J,K)=V(K,J)                                                      BJOR231
      L=L-1                                                              BJOR232
      IF(L.GT.1) GO TO 77                                                BJOR233
      DO 83 I=1,N                                                        BJOR234
      DO 82 J=1,N                                                        BJOR235
      K=NPV(J)                                                           BJOR236
   82 P(K)=V(I,J)                                                        BJOR237
      DO 83 J=1,N                                                        BJOR238
   83 V(I,J)=P(J)                                                        BJOR239
      DO 85 I=1,N                                                        BJOR240
      DO 84 J=1,N                                                        BJOR241
      K=NPV(J)                                                           BJOR242
   84 P(K)=V(J,I)                                                        BJOR243
      DO 85 J=1,N                                                        BJOR244
   85 V(J,I)=P(J)                                                        BJOR245
      DO 89 J=1,N                                                        BJOR246
      DO 89 I=1,N                                                        BJOR247
   89 V(I,J)=V(I,J)*DS                                                   BJOR248
      RETURN                                                             BJOR249
      END                                                                BJOR250
      FUNCTION ACPROD(AA,BB,N,CC)                                        BJOR251
C          THIS SUBROUTINE FORMS THE DOUBLE PRECISION PRODUCT OF THE     BJOR252
C          FIRST N VALUES OF THE ARRAYS, AA AND BB.  CC IS THEN ADDED IN BJOR253
C          DOUBLE PRECISION AND THE RESULT RETURNED IN SINGLE PRECISION  BJOR254
      DIMENSION AA(9),BB(9)                                              BJOR255
      DOUBLE PRECISION S,A,B,C                                           BJOR256
      S=0.D0                                                             BJOR257
      C=CC                                                               BJOR258
      DO 1 I=1,N                                                         BJOR259
      A=AA(I)                                                            BJOR260
      B=BB(I)                                                            BJOR261
    1 S=S+A*B                                                            BJOR262
      ACPROD=S+C                                                         BJOR263
      RETURN                                                             BJOR264
```

71 08 05

```
      END
         SCOPE
'LOAD
'RUN,2,10000,7
```

BJOR265